Single molecule counting detects low- copy glycine receptors in hippocampal and striatal synapses eLife Assessment

Peer-reviewed author version

Camuso, Serena; VELLA, Yana; Abadi, Souad; Mille, Clémence; BRONE, Bert & Specht, Christian (2025) Single molecule counting detects low- copy glycine receptors in hippocampal and striatal synapses eLife Assessment. In: eLife, 14 (Art N° RP109447).

DOI: 10.7554/eLife.109447.1
Handle: http://hdl.handle.net/1942/48612

eLife

Reviewed Preprint
v1 • December 15, 2025
Not revised

For correspondence:
christian.specht@inserm.fr

Competing interests: No competing interests declared

Funding: See page 20

Reviewing editor: Melike Lakadamyali, University of Pennsylvania, United States

Single molecule counting detects low-copy glycine receptors in hippocampal and striatal synapses

Serena Camuso[1], Yana Vella[2], Souad Youjil Abadi[1], Clémence Mille[1], Bert Brône[2], Christian G Specht[1]

[1]NeuroBicêtre, Inserm U1195, Université Paris-Saclay, Le Kremlin-Bicêtre, France • [2]UHasselt, Neurophysiology Laboratory, BIOMED research institute, Hasselt, Belgium

eLife Assessment

The study presents **convincing** quantitative evidence, supported by appropriate negative controls, for the presence of low-abundance glycine receptors (GlyRs) within inhibitory synapses in telencephalic regions of the mouse brain. Using sensitive single-molecule localization microscopy of endogenously tagged GlyRs, the authors reveal previously undetected populations of these receptors. Although the functional significance of these low-abundance GlyRs remains to be established, the findings offer **valuable** insights and methodologies that will be of interest to neuroscientists studying inhibitory synapse biology.

[Editors' note: this paper was reviewed by *Review Commons*.]

https://doi.org/10.7554/eLife.109447.1.sa4

Abstract

Glycine receptors (GlyRs) are heteropentameric chloride channels that mediate fast inhibitory neurotransmission in the brainstem and spinal cord, where they regulate motor and sensory processes. GlyRs are clustered in the post-synaptic membrane by strong interactions of the β subunit with the scaffold protein gephyrin. Even though GlyRβ mRNA is highly expressed throughout the brain, the existence of synaptic GlyRs remains controversial as there is little conclusive evidence using conventional fluorescence microscopy and electrophysiological recordings. Here we exploit the high sensitivity and spatial resolution of single molecule localisation microscopy (SMLM) to investigate the presence of GlyRs at inhibitory synapses in the brain, focusing on several areas of the telencephalon. Making use of a knock-in mouse model expressing endogenous mEos4b-tagged GlyRβ, we identified few GlyRs in sub-regions of the hippocampus. Dual-colour SMLM revealed that these sparse receptors are integrated within the post-synaptic gephyrin domain, pointing to a possible role in maintaining the structural integrity of inhibitory synapses. In contrast, we found functionally relevant numbers of synaptic GlyRs at inhibitory synapses in the ventral striatum. Our results highlight the strength of SMLM to detect few and sparsely distributed synaptic molecules in complex samples and to analyse their organisation with high spatial precision.

Introduction

Inhibitory neurotransmission in the central nervous system (CNS) is largely mediated by glycine receptors (GlyRs) and γ-aminobutyric acid type A receptors (GABAARs) (Alvarez, 2017, Kasaragod & Schindelin, 2018). Both classes of receptor are widely expressed throughout the brain and the spinal cord, however, they have specific regional expression patterns. GlyRs are particularly abundant in the spinal cord and brain stem, where they play an important role in the processing of sensory and motor information as well as the modulation of pain responses (Alvarez, 2017, Fenech et al., 2024). Although the expression of GlyRs is much lower in the brain

(Maynard et al., 2021, Zeilhofer et al., 2005), glycinergic transmission is known to be involved in reward signalling and possibly pain associated responses (Adermark et al., 2011, Devoght et al., 2023, Fenech et al., 2024, Muñoz et al., 2018, San Martin et al., 2020).

Both $GABA_A$Rs and GlyRs are cys-loop pentameric chloride channels that are composed of different combinations of subunits. Each subunit contains a large N-terminal extracellular domain (ECD), four transmembrane domains (TM1-4), as well as a flexible intracellular domain (ICD) between TM3 and TM4 (Kasaragod & Schindelin, 2018). Pentameric GlyRs are assembled from five different subunits, α1-α4 and β. Homopentameric GlyRs composed only of α subunits are mostly found in the extra-synaptic plasma membrane. In contrast, heteropentameric receptors containing both α and β subunits accumulate at post-synaptic sites, due to a direct interaction between the ICD of the β subunits and gephyrin, the main scaffold protein at inhibitory synapses (Alvarez, 2017).

In situ hybridisation studies have shown that the mRNA of the GlyRα1 and β subunits is highly expressed in spinal cord neurons (Ceder et al., 2024, Malosio et al., 1991). The GlyRβ transcript is also expressed in most brain regions, including olfactory bulb, cerebral cortex, hippocampus, and striatum (Ceder et al., 2024, Fujita et al., 1991, Malosio et al., 1991). Surprisingly, expression of GlyRβ protein appears to be exceedingly low in the telencephalon. For example, GlyR labelling was only detected at a few synapses in the hippocampus, mainly in the pyramidal layer (Danglot et al., 2004, Maynard et al., 2021, Weltzien et al., 2012). In line with this, electrophysiological measurements have failed to detect synaptic GlyR currents in the hippocampus (Chattipakorn & McMahon, 2002, Mori et al., 2002, Song et al., 2006), with only a single study reporting evoked IPSCs in mouse hippocampal CA1pyramidal cells (Muller et al., 2013).

The mRNA levels of the GlyR α subunits are generally low across the brain (Ceder et al., 2024, Malosio et al., 1991). Yet, surface expression of homopentameric GlyRs was demonstrated by electrophysiological recordings of glycine-induced currents in several regions including the hippocampus and dorsal striatum (Chattipakorn & McMahon, 2002, Comhair et al., 2018, Molchanova et al., 2017, Mori et al., 2002, Song et al., 2006). These extrasynaptic receptors are thought to play a role in the tonic inhibition of central neurons (McCracken et al., 2017, Mori et al., 2002, Song et al., 2006). This situation appears to be different in the ventral striatum (*nucleus accumbens*), where glycinergic mIPSCs likely corresponding to heteropentameric GlyRs have been reported (Muñoz et al., 2018), in addition to homopentameric receptors (McCracken et al., 2017, Molander & Söderpalm, 2005, Muñoz et al., 2020).

To explore the presence of GlyRs at synapses in the brain, we made use of the high spatial resolution and extraordinary sensitivity of single molecule localisation microscopy (SMLM), which enabled us to detect individual GlyR complexes in different regions of the telencephalon, including the hippocampal formation and striatum. Using a knock-in (KI) mouse model that expresses endogenous mEos4b-tagged GlyRβ subunits (Maynard et al., 2021), we identified low copy numbers of GlyRs at inhibitory synapses. Dual-colour SMLM further demonstrated the integration of these GlyRs within the post-synaptic gephyrin scaffold, suggesting that they are important for the assembly or maintenance of inhibitory synaptic structures in the brain.

Results

Identification of low-copy synaptic GlyRs in mouse hippocampus

The distribution of glycinergic synapses is mainly confined to the spinal cord and brain stem (Alvarez, 2017). While the presence of GlyRβ subunit mRNAs is well documented in different brain areas (Ceder et al., 2024, Fujita et al., 1991, Malosio et al., 1991); see also Supplementary Fig. S1), little is known about GlyRβ protein expression in the brain (Danglot et al., 2004, Maynard et al., 2021). Here, we exploited the high sensitivity and spatial resolution of SMLM to probe the presence of GlyRβ subunits at synapses in the brain, focusing on the hippocampus.

Since no reliable antibodies against the β-subunit of the GlyR are available, we used a knock-in mouse model expressing endogenous mEos4b-tagged GlyRβ subunits (Maynard et al., 2021, Wiessler et al., 2024). No obvious functional, behavioural or ultrastructural phenotypes have been reported in homozygous and heterozygous animals expressing mEos4b-GlyRβ. Thin cryostat coronal sections (10 µm) were cut from homozygous *Glrb*$^{eos/eos}$ mouse brain and labelled with NeuN antibody and with Sylite, a small peptide probe against the inhibitory synaptic scaffold protein gephyrin (Khayenko et al., 2022). The analyses were conducted in the molecular layer of the dentate gyrus (DG), where the dendrites of granule cells receive synaptic inputs from the entorhinal cortex, and in the *stratum radiatum* of the CA3 and CA1 regions, where the apical dendrites of pyramidal cells make contact with Mossy fibers and Schaffer collaterals, respectively (Supplementary Fig. S1C). The different hippocampal sub-regions were identified using the neuronal marker NeuN in the green channel (not shown). Reference images of Sylite were taken in the far-red channel, followed by SMLM recordings of the green-to-red photoconvertible fluorescent protein mEos4b attached to the GlyRβ subunit (Fig. 1A).

We observed very few single molecule detections during SMLM, indicating exceedingly low mEos4b-GlyRβ expression in the hippocampus. SMLM super-resolution images were reconstructed and analysed using Icy software to quantify the number of mEos4b detections per gephyrin cluster (Fig. 1B). We counted on average between 3 to 10 detections per synapse in all hippocampal sub-regions. This is about two orders of magnitude lower than in the spinal cord ($p < 0.0001$, non-parametric Kruskal-Wallis one-way ANOVA with Dunn's multiple comparison test, KW test), where we counted almost 1000 detections of mEos4b-GlyRβ per synapse (Fig. 1B, Supplementary Fig. S2). Aside from the low detection numbers in the hippocampus, we did not find obvious differences between the sub-regions, with a significant difference only between the DG and CA1 ($p = 0.002$, KW test).

To ascertain that what we saw in the hippocampus were indeed mEos4b detections and not imaging artefacts, we performed control experiments in hippocampal slices from wildtype mice not expressing mEos4b-tagged GlyRβ subunits. As expected, the mean number of detections at CA3 synapses was significantly lower in the negative control than in the *Glrb*$^{eos/eos}$ slices (Fig. 1B; $p < 0.0001$, KW test). Similarly, we recorded SMLM movies in *Glrb*$^{eos/eos}$ slices without 405 nm illumination. In the absence of UV, the mEos4b fluorescent protein is not converted into its red form, making this a stringent internal control. The number of detections per gephyrin cluster was again much lower than in the recordings with 405 nm laser illumination (Fig. 1B; $p < 0.0001$, KW). These data confirm that the non-specific background of detections, mainly outside of synapses, is sufficiently low to accurately identify and quantify endogenous mEos4b-GlyRβ subunits in the hippocampus of our knock-in mouse model. To exclude the possibility that the co-localisation between the mEos4b-GlyRβ detections and gephyrin was due to a random overlap, we did a pixel shift analysis with two-colour images of the CA3 region, in which the Sylite channel was horizontally flipped relative to the SMLM image of the mEos4b detections. This transformation led to a significant reduction in the number of mEos4b-GlyRβ detections at gephyrin clusters compared to the original data (Fig. 1B; $p < 0.0001$, KW), confirming that the localisation of mEos4b-GlyRβ at inhibitory synapses is not down to chance.

We also estimated the absolute number of GlyRs per synapse in the hippocampus. The number of mEos4b detections was converted into copy numbers by dividing the detections at synapses by the average number of detections of individual mEos4b-GlyRβ containing receptors. This value was measured across CA3 slices, both at synapses as well as in the extrasynaptic region (see Methods). The advantage of this counting strategy is that it is independent of the stoichiometry of heteropentameric GlyRs that is still under debate (e.g. (Durisic et al., 2012, Grudzinska et al., 2005, Patrizio et al., 2017, Zhu & Gouaux, 2021)). The obtained copy numbers are reported as background-subtracted values (Table 1). According to our quantification GlyRs are present at about a quarter of hippocampal synapses, with copy numbers most often in the single digits (Fig. 1C, Table 1). Only few synapses contain 10 or more GlyRs, and as many as 75% of hippocampal synapses do not contain any GlyRs at all. No obvious differences were noticed in the copy number of GlyRs between sub-regions. Taken together, our findings demonstrate the

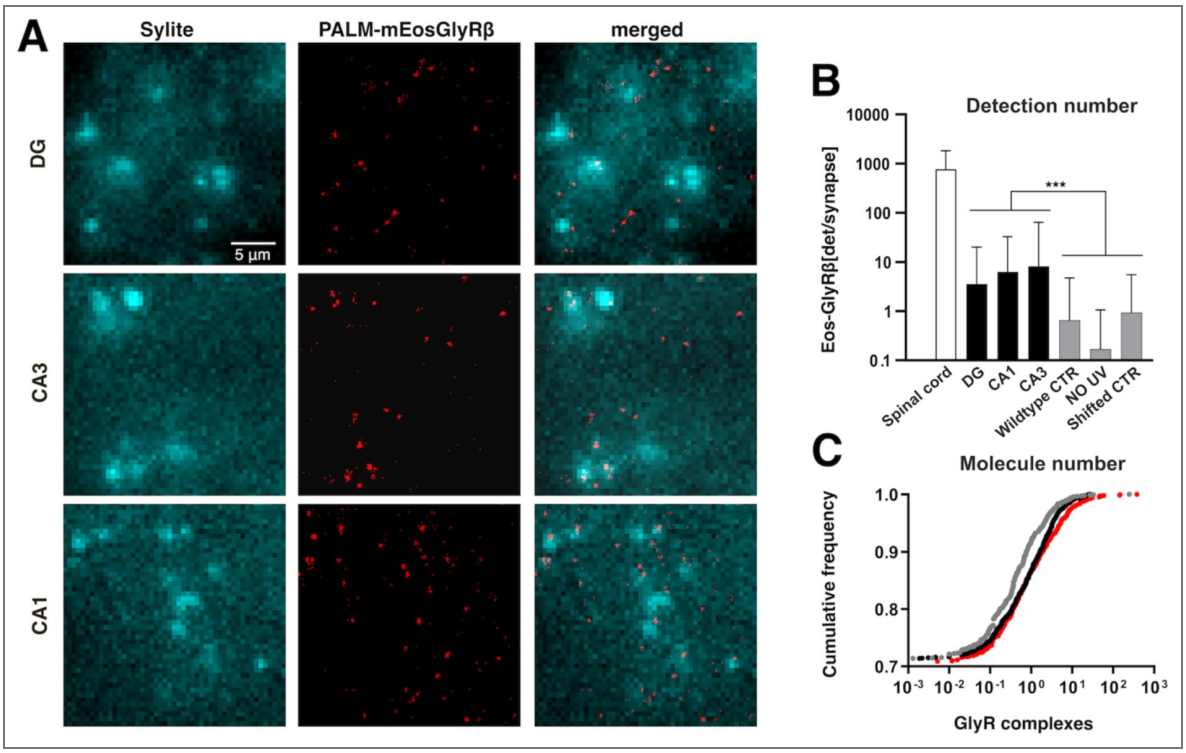

Figure 1. SMLM of mEos4b-GlyRβ subunits in the hippocampus.

(A) Single molecule detections of mEos4b-GlyRβ (red SMLM pointillist image) in the DG, CA1 and CA3 regions of the hippocampus in 10 µm cryostat sections of the knock-in mouse line *Glrb*$^{eos/eos}$ at postnatal day 40 (red pointillist images). Inhibitory synapses were identified in epifluorescence images using the gephyrin marker Sylite (cyan). Scale bar 5 µm. **(B)** Mean number of mEos4b-GlyRβ detections per synaptic gephyrin cluster in spinal cord (n = 9733 synaptic clusters from 10 fields of view) and brain slices (n > 5000 clusters from 9 fields of view for each region) from N = 3 independent experiments corresponding to three *Glrb*$^{eos/eos}$ mice. Recordings were also made in the CA3 of wildtype mice not expressing endogenous mEos4b-GlyRβ (negative control; n = 3637 clusters, 3 fields of view, 2 *Glrb*$^{WT/WT}$ mice) and in *Glrb*$^{eos/eos}$ hippocampal slices without photoconversion of mEos4b (no UV, n = 3301 clusters, 9 fields of view, 3 animals). A pixel shift control with flipped images was done with the same dataset (*Glrb*$^{eos/eos}$, CA3; n = 3301 clusters, 9 fields of view, 3 animals). Data are shown as mean ± SD. Levels of significance were determined using a Kruskal-Wallis test with Dunn's multiple comparison test: *** $p < 0.0001$. **(C)** Cumulative distribution representing the estimated copy number of mEos4b-GlyRβ complexes per synapse in DG (grey line), CA1 (black line) and CA3 (red line) regions. Copy numbers were background-corrected by subtracting the value obtained for the negative control in wildtype slices.

existence of very few heteropentameric GlyR complexes at inhibitory synapses in the hippocampus. With an average of approximately one GlyR per synapse, this is about a hundredfold lower than in the spinal cord.

Sub-synaptic distribution of GlyRs at hippocampal synapses

At glycinergic synapses in the spinal cord the receptors are anchored in the post-synaptic membrane by gephyrin, a scaffold protein that binds with high affinity to the GlyRβ subunit, promoting the synaptic localisation of GlyRs (e.g. (Kasaragod & Schindelin, 2018, Kostrz et al., 2024, Maynard et al., 2021)). The nanoscale organisation of inhibitory synapses in the hippocampus containing low-copy GlyRs has not yet been studied in detail (Danglot et al., 2004). To obtain information about the distribution of GlyRs within the synaptic structure, we carried out dual-colour SMLM of GlyRβ and gephyrin in brain slices of adult *Glrb*$^{eos/eos}$ mice using stochastic optical reconstruction microscopy (dSTORM) with organic fluorophores in a reducing buffer (Yang & Specht, 2020). Compared to SMLM with fluorescent proteins, dSTORM provides higher photon yields, resulting in a better localisation precision (~12 nm in our recordings, see Methods), which is critical for resolving fine structural details. For these experiments, we focused on the CA3 region of the hippocampus, where the presence of GlyRs at inhibitory synapses was demonstrated before (Fig. 1). Due to their low number, we did not expect to see any particular organisation of the receptors. Instead, the aim was to determine whether GlyRs are actually intrinsic components of the postsynaptic domain of inhibitory hippocampal synapses.

Endogenous mEos4b-GlyRβ subunits in tissue slices of *Glrb*$^{eos/eos}$ KI animals were labelled with anti-mEos-AF647 nanobodies (NanoTag). The specificity of the nanobody was tested in spinal cord slices that were also labelled with gephyrin antibody (mAb7a, Synaptic Systems) and a CF568-conjugated secondary antibody. Wide-field fluorescence images showed extensive co-localisation of all three channels (mEos4b, anti-gephyrin-CF568, anti-mEos-AF647) in *Glrb*$^{eos/eos}$ slices; the non-specific background of the nanobody in wildtype animals was very low (Supplementary Fig. S3).

For dual-colour SMLM, brain slices from *Glrb*$^{eos/eos}$ mice were labelled with anti-mEos-AF647 nanobody as well as with anti-gephyrin and CF680-conjugated anti-mouse secondary antibodies (Fig. 2A). The emitted light from the two far-red dyes was separated by spectral demixing, using a SAFe 360 nanoscope (Abbelight) equipped with a dichroic mirror at 700 nm and two sCMOS cameras for detection. In this imaging modality, the single molecule detections recorded simultaneously on the two cameras are attributed to one or the other far-red fluorophore based on their specific intensity ratio (see Methods; Supplementary Fig. S4A-E). To further test the specificity of the nanobody labelling and the demixing procedure, we performed experiments in *Glrb*$^{eos/eos}$ slices in which the nanobody was omitted and only gephyrin was labelled (CF680). Under these conditions, spectral demixing produced a single peak of intensity ratios corresponding to the CF680 fluorophore, with only few wrongly attributed detections in the AF647 channel (Supplementary Fig. S4F,G).

In line with our SMLM experiments with the photoconvertible fluorescent protein mEos4b in brain slices (Fig. 1), we observed sparse single molecule detections of anti-mEos-AF647 nanobody that generally co-localised with dense clusters of gephyrin detections, confirming the presence of mEos4b-GlyRβ at inhibitory synapses in the hippocampus (Fig. 2A). The two-colour SMLM pointillist images were analysed using the DBSCAN clustering tool in the NEO software to measure the distance between mEos4b-GlyRβ and the corresponding gephyrin clusters. According to our measurements, the Euclidean distance between the centre of mass (CM) of GlyRβ and gephyrin was 80 ± 69 nm (mean ± SD, n = 214 pairs of clusters), pointing to a close spatial relationship at inhibitory synapses (Fig. 2B). We also calculated the relative distance of the GlyRβ detections from the centre of mass of gephyrin, compared to the mean distance of the gephyrin detections from their own centre of mass as defined by the radius of gyration (RG) of the gephyrin clusters. This ratio was below one for most clusters, indicating that the GlyRs are well integrated within the postsynaptic gephyrin domains at CA3 synapses (Fig. 2C).

Table 1. Estimated copy numbers of mEos4b-GlyRβ containing heteropentameric GlyR complexes at inhibitory synapses in different regions of the CNS of *Glrb*$^{eos/eos}$ KI mice (background-corrected, see Methods).

CNS region	GlyR copy number (mean ± SEM)	range of GlyR copies (5-95 percentile)	fraction of GlyR positive synapses (≥ 0.5 copies)
Spinal cord	120 ± 5	0 – 470	0.89
CA1	0.34 ± 0.05	0 – 3	0.18
CA3	1.11 ± 0.30	0 – 5	0.18
DG	0.35 ± 0.18	0 – 2	0.13
Dorsal striatum	3.00 ± 0.18	0 – 15	0.43
Ventral striatum	26.10 ± 1.48	0 – 112	0.73

Figure 2. Dual-colour SMLM of GlyR and gephyrin at inhibitory hippocampal synapses.

(A) Dual-colour SMLM using spectral demixing of endogenous mEos4b-GlyRβ labelled with anti-mEos-AF647 nanobody (red, NanoTag), and mouse anti-gephyrin (mAb7a, Synaptic Systems) and CF680-conjugated secondary anti-mouse antibodies (cyan) in hippocampal slices of the *Glrb*$^{eos/eos}$ knock-in mouse line at postnatal day 40. Scale: 500 nm. **(B)** Euclidean distance between the centre of mass (CM) of the anti-mEos-AF647 nanobody (GlyRβ) and gephyrin (mAb7a-CF680) detections of corresponding clusters. **(C)** Distance of the CM of the anti-mEos-AF647detections from the CM of gephyrin relative to the radius of gyration (RG) of the gephyrin cluster along the x and y axes (Δx/RGx, Δy/RGy). N = 2 independent experiments corresponding with 2 *Glrb*$^{eos/eos}$ animals.

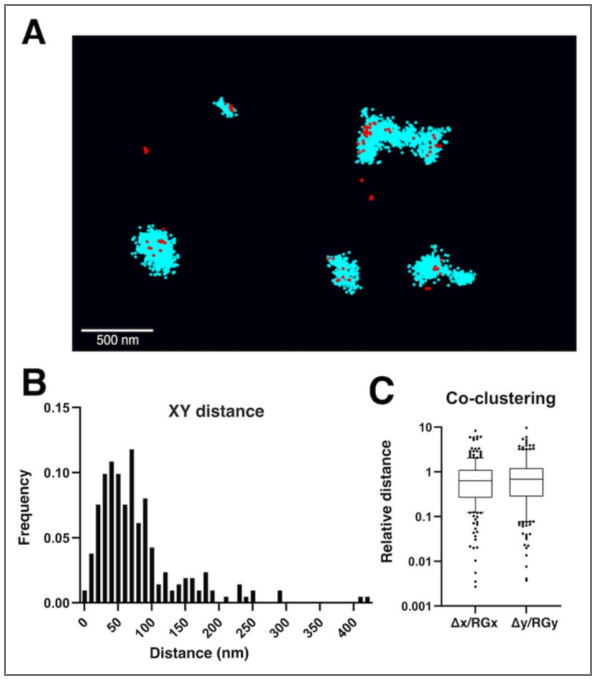

Differential expression of endogenous mEos4b-GlyRβ in dorsal and ventral striatum

Several reports have described the presence of glycinergic currents in the striatum (Molchanova et al., 2017, Muñoz et al., 2018). However, the localisation of GlyRs at synapses in this brain area remains controversial. Homopentameric GlyRα2 complexes are thought to mediate tonic inhibition in the dorsal striatum (Devoght et al., 2023, Molchanova et al., 2017), yet glycinergic miniature inhibitory postsynaptic currents (mIPSCs) were detected in the *nucleus accumbens*, i.e. part of the ventral striatum (Muñoz et al., 2018). To resolve this issue, we quantified the GlyRβ-containing synaptic receptors in the striatum of $Glrb^{eos/eos}$ animals using SMLM.

The number of detections of mEos4b-GlyRβ per gephyrin cluster, as well as the resulting copy number of GlyRs at synapses were measured in the dorsal and in the ventral striatum in $Glrb^{eos/eos}$ mice at postnatal day 40. Coronal cryo-sections of 10 µm thickness were immunolabeled for NeuN to distinguish the two sub-regions of the striatum. Gephyrin was labelled with the Sylite probe in order to identify inhibitory synapses (Fig. 3A). The average number of mEos4b-GlyRβ detections per gephyrin cluster was significantly higher in the ventral striatum compared to the dorsal striatum (136 ± 5 versus 25 ± 1 detections per synapse, mean ± SEM, n = 3309 and 2352 synapses, respectively; $p < 0.0001$, non-parametric Mann-Whitney test, MW test; Fig. 3B). Conversion of the detection numbers into receptor copy numbers revealed that about 40% of synapses in the ventral striatum contain at least 10 heteropentameric GlyR complexes, many more than in the dorsal striatum ($p < 0.0001$, KW test; Fig. 3C, Table 1). As before, copy numbers are given as background-corrected values (see Methods). The same quantification was done in the spinal cord, where we found significantly higher copy numbers of receptor complexes containing mEos4b-GlyRβ ($p < 0.0001$ against both striatal regions, KW). With an average of 120 ± 5 receptor complexes per synaptic cluster (mean ± SEM, n = 4006 synapses, Table 1), these values are close to previous estimates (Maynard et al., 2021).

Our findings show that the numbers of mEos4b-GlyRβ subunits are much higher at synapses in the striatum compared to synapses in the hippocampal formation, and that their distribution in the striatum is area-specific. This observation is supported by electrophysiological recordings of glycinergic synaptic currents in the *nucleus accumbens* (Muñoz et al., 2018) as opposed to mainly extrasynaptic tonic currents in the dorsal striatum (Molchanova et al., 2017).

Miniature synaptic currents in ventral striatum recorded with whole cell patch-clamp

Since the published recordings of glycinergic currents in the striatum were performed under different conditions, i.e. different striatal sub-regions, mouse strains and ages (Molchanova et al., 2017, Muñoz et al., 2018), we wanted to verify the area-specific functional differences in a single experimental setting. We pharmacologically isolated glycinergic mIPSCs and determined their frequency and amplitudes in brain slices of both ventral and dorsal striatum of C57BL/6J mice at postnatal day 35 to 41 using whole cell patch clamp (Fig. 4). mIPSCs are considered a measure of functional synapses because they are generated by the spontaneous release of synaptic vesicles from presynaptic terminals. Our data confirm the presence of glycinergic mIPSCs in medium spiny neurons (MSNs) in the ventral striatum and the near complete absence of glycinergic mIPSCs in dorsal striatal MSNs ($p < 0.05$, MW test; Fig. 4D). With an amplitude of 17.2 ± 2.9 pA (mean ± SEM, n = 5 cells from N = 3 animals; Fig. 4C) and a frequency of 0.12 ± 0.03 Hz (Fig. 4D), the mIPSCs recordings in the ventral striatum are similar to the results of an earlier study of the *nucleus accumbens* (Muñoz et al., 2018). Our electrophysiological data also match the differences in synaptic GlyR copy numbers obtained by quantitative SMLM (Fig. 3C).

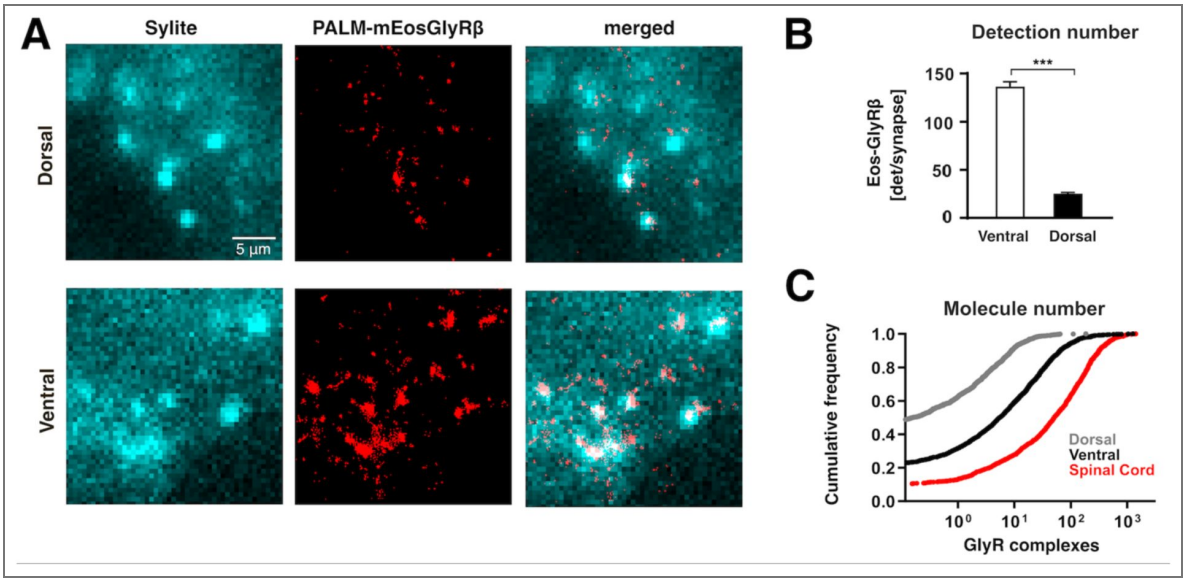

Figure 3. Quantitative SMLM of endogenous GlyRs at synapses in the striatum.

(A) Super-resolution imaging of mEos4b-GlyRβ subunits (in red) in the dorsal and ventral striatum of *Glrb*$^{eos/eos}$ knock-in mice. Cryostat slices were labelled with the gephyrin marker Sylite (cyan). Scale: 5 µm. **(B)** Single molecule detection numbers of mEos4b-GlyRβ per gephyrin cluster (n = 3309 and 2352 clusters for ventral and dorsal striatum, respectively, from 9 fields of view per sub-region and N = 3 independent experiments from three animals; mean ± SEM; two-tailed Mann-Whitney test: *** $p < 0.0001$). **(C)** Cumulative distribution of the estimated number of mEos4b-GlyRβ containing receptor complexes per synapse in the dorsal striatum (grey line), ventral striatum (black line) and spinal cord (red line). Copy numbers are background corrected (see Table 1).

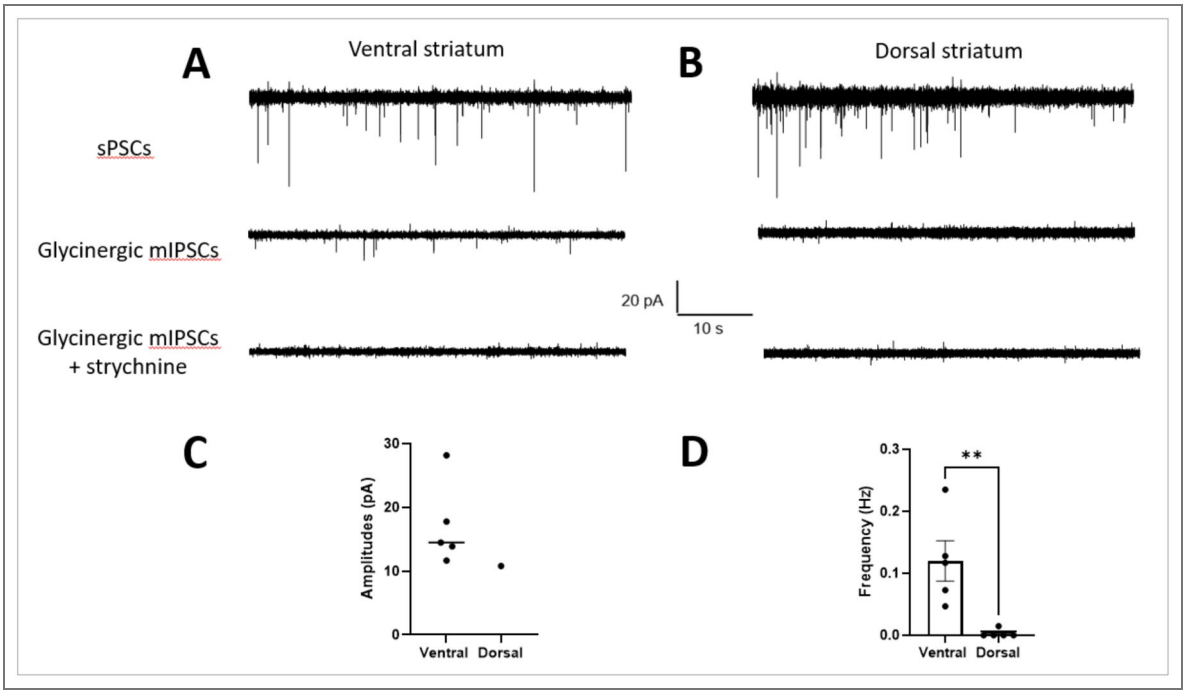

Figure 4. Glycinergic mIPSCs of MSNs in ventral but not in dorsal striatum.

(A-B) Representative ventral and dorsal current traces recorded using whole cell patch clamp in medium spiny neurons (MSNs) in the ventral (A) and dorsal striatum (B). The top traces show spontaneous postsynaptic current (sPSCs) recorded during aCSF application to confirm whole cell recording. The middle traces show the pharmacologically isolated glycinergic mIPSCs during the application of aCSF containing blockers (10 μM DNQX, 0.1 μM DHBE, 5 μM L-689560, 0.5 μM tetradotoxin, and 10 μM bicuculline) present in the ventral striatum and absent in dorsal striatum. Blocking the mIPSCs by 1 μM strychnine confirms their glycinergic identity. **(C)** Quantification of the amplitude and **(D)** frequency of glycinergic mIPSCs in ventral and dorsal MSNs (mean ± SEM; n = 5 cells from 3 animals in ventral striatum and n = 5 cells from 4 animals in dorsal striatum). Levels of significance determined using a one-tailed Mann-Whitney test (** $p < 0.05$).

Expression of recombinant GlyR subunits in cultured hippocampal neurons

Synaptic GlyRs are heteropentamers composed of α (α1–α4) and β subunits, and their assembly and synaptic targeting requires the presence of both types of subunit (Alvarez, 2017). Since the β transcript appears to be highly expressed in most neurons including in the hippocampus (Supplementary Fig. S1), we hypothesised that the expression of α subunits could be the limiting factor controlling the number of synaptic GlyRs. We therefore expressed different recombinant GlyR subunits in cultured hippocampal neurons and analysed their accumulation at inhibitory synapses.

Cells were transduced with lentivirus expressing mEos4b-tagged GlyR α1, α2 or β at day *in vitro* 3 (DIV3), fixed at DIV16, and stained with Sylite to identify synaptic gephyrin clusters. We observed co-localisation of mEos4b and Sylite puncta in neurons infected with either of the virus constructs, indicating that some cultured hippocampal neurons express the corresponding endogenous α or β subunits (Fig. 5A). However, synaptic GlyR puncta were not found in all neurons despite using high virus titres. This means that low levels of α and/or β mRNA transcripts in hippocampal neurons can limit the expression of heteropentameric GlyRs. Interestingly, the mEos4b-GlyRα1 construct was expressed at a higher rate than of the other subunits and had a punctate appearance in most neurons (Fig. 5A). The majority of these puncta co-localised with gephyrin, implying the assembly of mixed GlyRs composed of recombinant mEos4b-GlyRα1 and endogenous GlyRβ subunits. We occasionally also observed mEos4b-GlyRα1 puncta that did not co-localise with gephyrin. These are likely clusters of homopentameric receptors in the extrasynaptic membrane, similar to the clustering of GlyRα3L homopentamers reported in HEK 293 cells (Notelaers et al., 2012). In contrast to GlyRα1, expression of GlyRα2 produced a diffuse labelling in most infected neurons with only weak synaptic puncta. The distribution of recombinant GlyRs at synapses and in the extrasynaptic membrane was confirmed by SMLM imaging of the mEos4b-tagged receptor subunits (Fig. 5B). In line with the above observations, we found a mainly clustered distribution of GlyRα1, both at synapses as well as in the extrasynaptic membrane. The GlyRα2 subunit had a large extrasynaptic receptor population, likely composed of diffusely distributed GlyRα2 homopentamers, and only few synaptic heteropentamers. The mEos4b-GlyRβ subunit was visibly expressed only in a few cells, where it had a predominantly synaptic localisation as a result of its direct interaction with gephyrin.

For a more systematic evaluation of the sub-cellular distribution of the GlyRs, we counted the percentage of infected neurons in which a synaptic localisation of the recombinant receptor subunits could be seen in the merged epifluorescence images (Fig. 5C, see Methods). Essentially all GlyRα1 infected neurons had mEos4b-positive gephyrin clusters, indicating a robust synaptic localisation of the α1 subunit. From this can be deduced that most if not all hippocampal neurons express endogenous GlyRβ transcripts. When the cultures were infected with mEos4b-GlyRβ, only few neurons showed a synaptic localisation, meaning that there are only few endogenous α subunits available and that they constitute the limiting factor for synaptic targeting. Interestingly, very few mEos4b-GlyRα2 expressing neurons displayed synaptic localisation, which suggests that not all α subunits are equally capable of forming heteropentameric GlyR complexes with endogenous β subunits.

We also quantified the total intensity of mEos4b-tagged GlyRα1, α2 and β at synaptic gephyrin clusters in infected hippocampal neurons and uninfected control cultures (Fig. 5D). Consistent with our previous observations, mEos4b-GlyRα1 accumulated strongly at inhibitory synapses, again pointing to efficient synaptic targeting. GlyRα2 and GlyRβ subunits showed lesser accumulation at synapses. Pairwise comparison between mEos4b-GlyRα1 and mEos4b-GlyRα2 expressing neurons using a non-parametric Mann-Whitney test showed that the mean total intensity of synaptic GlyRα1 is significantly higher than that of GlyRα2 ($p < 0.01$, MW test). Although the total intensity of the Sylite puncta was not significantly different between conditions when all groups were compared (Fig. 5E; KW test), a pairwise comparison between mEos4b-GlyRα1 expressing neurons and uninfected controls showed a significant increase in Sylite

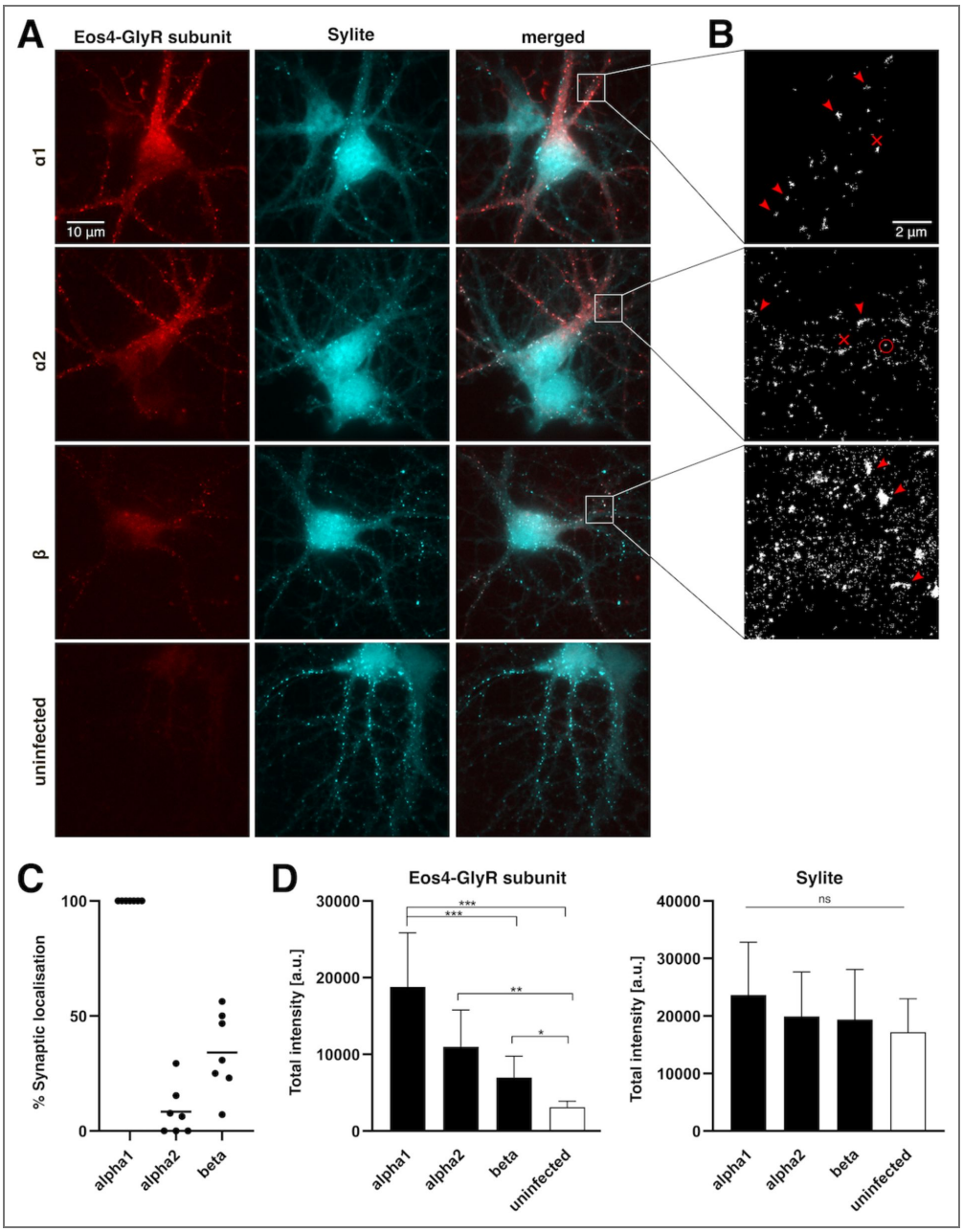

Figure 5. Expression of recombinant GlyR subunits in cultured hippocampal neurons.

(A) Cultured mouse embryonic hippocampal neurons (E17.5) were transduced with lentivirus expressing mEos4b-tagged GlyR subunits α1, α2 or β (red), fixed at DIV17 and stained for gephyrin (Sylite marker, cyan). Bottom images: uninfected control neurons. Scale: 10 µm. **(B)** SMLM pointillist images showing the photoconverted mEos4b detections. Dense clusters of synaptic (red arrowheads) and extrasynaptic receptors (red crosses) are indicated. Diffusely distributed extrasynaptic GlyR complexes (red circle) are seen as small clusters of detections resulting from the repetitive detection of a single mEos4b fluorophore. Scale: 2µm. **(C)** Quantification of the percentage of infected neurons displaying mEos4b-positive GlyR clusters that co-localise with synaptic gephyrin clusters. Each data point represents one coverslip of cultured neurons (n = 7 coverslips per condition, corresponding to 105 cells for GlyRα1, 114 cells for GlyRα2, and 109 cells for GlyRβ, from N = 4 independent experiments (i.e. cultures). The mean is indicated as horizontal line. **(D)** Quantification of the total fluorescence intensity of mEos4b-tagged GlyR subunits at Sylite puncta in infected neurons and uninfected controls. The integrated mEos4b fluorescence (left graph) and integrated Sylite fluorescence (right) was measured for every Sylite-positive punctum and the median calculated per cell (n = 21 cells for GlyRα1; 9 for GlyRα2; 33 for GlyRβ, and 18 control cells, from N= 3 experiments; mean ± SD; KW test. *p < 0.05; ***p < 0.01; ***p < 0.0001; n.s. not significant). The camera offset was corrected using the minimum pixel intensity in each channel. The signal in the mEos4b channel in the control cultures represents the fluorescence background.

labelling ($p < 0.05$, MW test). This seems to indicate that enhanced expression of GlyRα1/β heteropentamers can augment the size of the postsynaptic gephyrin scaffold at inhibitory synapses in the hippocampus.

Discussion

Detection of heteropentameric GlyR complexes at hippocampal synapses using SMLM

Making use of the outstanding sensitivity of single molecule localisation microscopy (SMLM) this study describes the presence of very low copy numbers of GlyRs at synapses throughout the hippocampus. Key to this was the use of highly specific labelling of synaptic receptors using a knock-in mouse model expressing endogenous mEos4b-GlyRβ that was used either directly for SMLM through the photoconversion of the mEos4b fluorescent protein or as an antigen that was recognised by a specific anti-mEos nanobody. To positively identify the GlyRβ signals, it was necessary to reduce as much as possible the non-specific background of detections that invariably occurs in SMLM recordings. In the case of mEos4b imaging, this was done by acquiring a negative control movie without photoconversion of the fluorophore. In other words, the photo-physical properties of the fluorophore can be used to identify them with some certainty (Wulffele et al., 2022). Since we focussed on GlyRs at inhibitory synapses, the co-localisation of the detections with the synaptic gephyrin scaffold provided additional assurance that single mEos4b fluorophores could be identified in 10 µm thick slices of brain tissue. These data illustrate the power of SMLM to detect rare or sparsely distributed target molecules in complex samples, in addition to the high spatial precision afforded by super-resolution imaging.

Another strength of SMLM is the possibility to gain access to absolute molecule numbers. Since a fluorophore can be detected several times during the recording, the number of detections has to be translated into the number of emitting fluorophores (Patrizio & Specht, 2016). This is generally more straightforward with fluorescent proteins such as mEos4b that are irreversibly bleached after a number of detections (Wulffele et al., 2022), instead of organic fluorophores (e.g. AF647) that can blink over extended periods. In our case, the use of a knock-in mouse ($Glrb^{eos/eos}$) expressing recombinant mEos4b-GlyRβ made it possible to calculate the copy number of endogenous GlyRs at synapses (Maynard et al., 2021). To ensure accurate readings, SMLM movies were recorded until all fluorophores were exhausted (typically 5000 frames in hippocampus and as many as 15000 in the spinal cord, see Methods). Even so, the obtained values have to be taken as estimates given the stochasticity of the number of detections per mEos4b fluorophore.

Our quantification in spinal cord slices indicated that there are on average 120 GlyRs per synapse (Table 1). This result is similar to earlier measurements, in which we calculated median values of 114 and 238 GlyRs at synapses in the dorsal and the ventral horn of the spinal cord, respectively (Maynard et al., 2021). The slightly lower values compared to the earlier study could be related to the lower age of the animals (40 days instead of 2 or 10 months), or to the greater thickness of the sample (10 µm versus 2 µm slices) that affects the signal to noise ratio of the detections. Furthermore, a simpler approach was used in the current study to translate detections into copy numbers. We divided the number of detections at synapses by the number of clusters of detections in sparsely labelled regions in the CA3 that contain mostly individual and spatially separated GlyRs (including extrasynaptic receptors). The advantage of this estimation is that it is independent of the stoichiometry of heteropentameric GlyRs that remains controversial (e.g. (Durisic et al., 2012, Durisic et al., 2014, Grudzinska et al., 2005, Maynard et al., 2021, Patrizio et al., 2017, Yu et al., 2021, Zhu & Gouaux, 2021)). However, our quantification could underestimate the GlyR copy numbers, because a certain fraction of fluorescent proteins like mEos4b is often not functional or not detected under the given imaging conditions, partly due to their complex photo-physical properties (e.g. (Durisic et al., 2014, Patrizio et al., 2017, Wulffele et al., 2022).

As opposed to spinal cord synapses, the numbers of GlyRs at hippocampal synapses are very low. In most cases, only a single cluster of detections (i.e. a single heteropentameric GlyR complex) was present at these synapses (Table 1). Yet, the existing GlyRs appear to be well integrated into the gephyrin domain as judged by dual-colour super-resolution microscopy, pointing to a possible role at synapses (see below).

Discrepancies between transcription and protein expression of GlyRs in the brain

Our study addresses a long-standing debate about the presence of GlyRs in the brain. According to many reports including recent transcriptomic analyses, GlyRβ mRNA is highly expressed in neurons throughout the telencephalon including the hippocampus (Ceder et al., 2024, Fujita et al., 1991, Malosio et al., 1991) (see also Fig. S1). For instance, ISH data from mouse brain show strong GlyRβ signals in the CA1 neurons consistent with elevated transcription of GlyRβ in pyramidal cells (Allen brain atlas, *http://mouse.brain-map.org/gene/show/14434*). This is also true for the human brain, where high GlyRβ mRNA levels are detected in all sub-regions of the hippocampus (*https://www.proteinatlas.org/ENSG00000109738-GLRB/brain*; (Karlsson et al., 2021)). In spite of this, the protein expression of GlyRβ receptor subunits in the hippocampus is very low, as judged by our analysis of synaptic (heteropentameric) GlyRs in mEos4b-GlyRβ knock-in animals. What, then, is the reason for the low protein expression of GlyRβ?

A likely explanation is that the assembly of mature heteropentameric GlyRs depends critically on the co-expression of endogenous GlyR α subunits. The presence of transcripts of the GlyR subunits α1, α2 and α3 in the brain has been demonstrated (Ceder et al., 2024, Malosio et al., 1991), in line with the existence of extrasynaptic (homopentameric) GlyR complexes (Chattipakorn & McMahon, 2002, Molchanova et al., 2017, Mori et al., 2002, Song et al., 2006). Our re-analysis of transcriptomic data confirms that the GlyRα1 mRNA levels are low in the telencephalon, and increase towards dorsal regions of the brain (Fig. S1A), in parallel with the expression of GlyRβ protein and its localisation at inhibitory synapses (Maynard et al., 2021). This raises the interesting possibility that heteropentameric assembly and subsequent synaptic targeting of GlyRs may depend specifically on the concomitant expression of both, α1 and β transcripts. To test this hypothesis, we expressed recombinant GlyR α and β subunits in cultured hippocampal neurons. Lentiviral expression of mEos4b-GlyRβ resulted in synaptic receptors only in some cells, suggesting that in the majority of the neurons the β transcript is not the limiting element for cell-surface delivery and synaptic targeting of heteropentameric GlyR complexes. In contrast, lentiviral infection with an mEos4b-GlyRα1 construct resulted in efficient surface expression of GlyRα1 clusters in hippocampal neurons, where it generally co-localised with the synaptic gephyrin scaffold. In contrast, mEos4b-GlyRα2 was mostly extrasynaptic and less often and less strongly present at synapses. These observations indicate that GlyRα1 (and possibly GlyRα3) could have a particular role in the assembly and forward trafficking of heteropentameric GlyRs towards the plasma membrane.

Our analyses also showed that lentivirus infection did not alter the gephyrin cluster intensities in hippocampal neurons, suggesting that long-term expression of GlyR subunits does not affect the size of inhibitory synapses *per se*. However, the expression of mEos4b-GlyRα1 led to a slight increase in total gephyrin intensity. In our view, this is the result of the increased expression of GlyRα1/β heteropentamers and their accumulation at inhibitory synapses, which in turn can recruit additional gephyrin molecules to the postsynaptic scaffold.

Possible roles of low-copy GlyRs at brain synapses

The low number of GlyRs at hippocampal synapses begs the question what their role may be. Experiments in GlyRα2 knock-out animals have shown that GlyRs help maintain the excitatory / inhibitory balance in the dorsal striatum (Devoght et al., 2023). However, these receptors are likely to be extrasynaptic GlyRα2 homopentamers. On the other hand, the contribution of a single synaptic GlyR to the chloride influx during inhibitory neurotransmission is probably not significant. In line with this interpretation, glycinergic miniature IPSCs in hippocampal slices are

not generally detected (Chattipakorn & McMahon, 2002, Mori et al., 2002, Song et al., 2006), but see (Muller et al., 2013)). The same is true for the *putamen* (dorsal striatum), where whole-cell currents were recorded in response to glycine application (Molchanova et al., 2017). Again, our quantification indicates that GlyR copy numbers in this area are low (Table 1). Synaptic GlyRs are more numerous at synapses in the *nucleus accumbens* (ventral striatum), and indeed, our electrophysiological data support this finding in agreement with earlier studies (Muñoz et al., 2018).

Another possible role of low-copy GlyRs at synapses in the hippocampus, dorsal striatum and maybe other regions of the telencephalon could be a structural one. This concept is based on the high affinity of the GlyRβ-gephyrin interaction (Kasaragod & Schindelin, 2018) that stabilises the receptor as well as the gephyrin scaffold at inhibitory synapses (Chapdelaine et al., 2021). Accordingly, overexpression of synaptic GlyRα1/β heteropentamers led to an increase in gephyrin levels at hippocampal synapses (Fig. 5D). Our two-colour SMLM data of endogenous mEos4b-GlyRβ and gephyrin at hippocampal synapses further confirm that despite their low number the GlyRs are integral components of the postsynaptic gephyrin domain in support of a structural role. $GABA_AR$ subunits have a much lower affinity for gephyrin and cannot provide the same level of stability (e.g. (Kostrz et al., 2024, Maric et al., 2014, Maric et al., 2011)). However, $GABA_ARs$ could probably be recruited efficiently to an existing gephyrin scaffold.

In conclusion, our data positively identify the presence of very small numbers of heteropentameric GlyRs at inhibitory synapses in the brain. This is drastically different to the situation in the *nucleus accumbens*, and even more so in the spinal cord, where GlyRs are abundant and densely clustered at most inhibitory synapses. While it is reasonable to classify different inhibitory synapses as mainly glycinergic or GABAergic, it should be noted that this is a simplification that does not account for the full diversity of inhibitory synapses that may assemble in a continuum of mixed compositions across the entire dynamic range.

Methods

Primary culture of hippocampal neurons

Hippocampal neurons were prepared from wild-type mice with Swiss background, at embryonic day E17.5. Experiments were performed according to the European directive on the protection of animals used for scientific purposes (2010/63/EU) and the regulations of the local veterinary authority (Inserm UMS44-Bicêtre, license G94043013). The mice came from excess production for another project, meaning that no animals were generated for the current project.

Pregnant mice were put to death by cervical dislocation and the embryos collected by caesarean section and decapitated. Hippocampi were rapidly dissected in cold Hank's Balanced Salt Solution (HBSS, Gibco, #14180-046) containing 20 mM HEPES (Gibco, #15630-056) and incubated at 37°C for 15 min in dissection medium containing 0.25% trypsin (Gibco #15090-046). After trypsinisation, hippocampi were washed twice in plating medium composed of Minimal Essential Medium (MEM) containing Earle's Balanced Salts (EBSS) (Cytiva, #SH30244.01), 2 mM GlutaMAX (Gibco, #35050-038), 1 mM sodium pyruvate (Thermo Fisher Scientific, #11360-039), and 10% heat inactivated horse serum (Gibco, #26050-088). The hippocampal tissue was then triturated in plating medium containing 0.3 mg/ml DNase I (Merck, #11284932001). Neurons were seeded at a concentration of $3.4 \times 10^5/cm^2$ in 12-well plates (Thermo Fisher, #150628) on round glass coverslips (type 1.5, 18 mm diameter; Marienfeld, #0112580) that were pre-coated with poly-D,L-ornithine (Merck, #P8638). The medium was replaced 4 hours after plating with maintenance medium: Neurobasal medium (Gibco, #21103-049) containing B-27 Supplement (Gibco, #17504-044) and 2 mM GlutaMAX. Once a week, 300 µL of fresh maintenance medium was added. Hippocampal neurons were typically infected with ≤ 50 µl of lentivirus stocks at DIV3 (FU-mEos4b-GlyRα2, FU-mEos4b-GlyRβ) or DIV10 (FU-mEos4b-GlyRα1) and fixed for immunocytochemistry at day *in vitro* DIV16.

Lentivirus expression constructs

The following lentivirus constructs were used for the expression of mEos4b-tagged GlyR subunits: FU-mEos4b-GlyRα1, expressing the coding sequence (cds) of rat *Glra1* isoform a (UniProt P07727-1) (Patrizio et al., 2017); and FU-mEos4b-GlyRβ-bis the cds of human GLRB (UniProt P48167-1) (Grunewald et al., 2018). The receptor sequence in construct FU-mEos4b-GlyRβ-bis (excluding the signal peptide and mEos4b sequence) was replaced with the cds of human GLRA2 (UniProt P23416) to generate the expression construct FU-mEos4b-GlyRα2.

For virus production, HEK-293 tsA201 cells were co-transfected with equal amounts (5 µg each) of the replicon plasmid and the three helper plasmids pMDLg/pRRE, pRSV-Rev, and pMD2.G (Addgene #12251, #12253, #12259) using lipofectamine 2000 (Invitrogen, #11668-019). Cells were cultured in maintenance medium (see above) supplemented with 5 U/ml penicillin and 5 µg/ml streptomycin at 37°C / 5% CO_2 for 24 h, at which point the medium was exchanged. The culture medium containing lentivirus was collected at 48-55 hours, filtered with a pore size of 0.45 µm, and frozed as aliquots at -70°C.

Immunocytochemistry in cultured neurons

Hippocampal neurons were fixed at DIV16 with 4% w/v PFA and 1% w/v sucrose in 0.1 M phosphate buffer (PB), pH 7.4 for 10 min. After three washes in PBS, the cells were permeabilized in PBS, pH 7.4 containing 0.25% Triton X-100 and 4% w/v bovine serum albumin (BSA) (Sigma, #A7030) for 10 min and then blocked in PBS containing 4% w/v BSA for 1 h. Neurons were incubated for 1h with the 200 nM of the gephyrin marker Sylite (Khayenko et al., 2022) in PBS containing 1% w/v BSA. The cells were rinsed twice in PBS and kept in PBS overnight at 4°C until imaging.

Sample preparation of spinal cord and brain slices for SMLM of endogenous mEos4b-GlyRβ

Brain and spinal cord tissue from homozygous mEos4b-GlyRβ knock-in (KI) mice (*Glrb*$^{eos/eos}$, mouse strain C57BL/6N-*Glrb*^{tm1Ics}, backcrossed into C57BL/6J, accession number MGI:6331106 (Maynard et al., 2021)) was recovered from an earlier project (Wiessler et al., 2024). In this mouse strain the β-subunit of the GlyR is tagged at its N-terminus with the photoconvertible mEos4b fluorescent protein. The chosen animals did not carry any genomic modification other than *Glrb*$^{eos/eos}$. For control experiments brain tissue from a wild-type Swiss mouse was used. Freshly frozen spinal cords and brains from male and female mice at postnatal day 40 were embedded in OCT (Pink Neg-50, Thermo Fisher Scientific, #6502P) and coronal slices of a nominal thickness of 10 µm were cut on a cryostat (Leica, Wetzlar, Germany, #CM3050S) with a chamber temperature of -23°C. The slices were collected on SuperFrost Plus glass slides (Epredia, #J7800AMNZ), fixed with 2% w/v PFA and 0.5% w/v sucrose in PB, pH 7.4 for 10 min and rinsed three times for 5 min in PBS at room temperature (RT). Afterwards, the slices were permeabilized and blocked in PBS containing 4% w/v BSA (A7030, Sigma) and 0.25% v/v Triton X100 for 15 min. Optionally, the slices were labelled overnight with a polyclonal antibody against NeuN (raised in chicken, Synaptic Systems, #266006, 1:2000) at 4°C, followed by 4 h of AF488-conjugated donkey anti chicken secondary antibody (Jackson ImmunoResearch, #703-545-155, 1:2000) at RT. The gephyrin-specific peptide probe Sylite (Khayenko et al., 2022) was applied at a final concentration of 50 nM in PBS containing 1% w/v BSA for 1 h at RT. After two washes of 5 min in PBS, slices were mounted in PBS, covered with a glass coverslip (type 1.5), sealed with PicoDent Twinsil Speed (#1300-1002) and kept overnight at 4°C or directly used for SMLM imaging of the mEos4b photoconvertible protein.

Single molecule localisation microscopy (SMLM) of mEos4b fluorescent protein

SMLM imaging of mEos4b-tagged GlyRs was performed using an ELYRA PS.1 microscope setup (Zeiss, Jena, Germany). Samples were placed on the motorized stage of an Axio Observer.Z1 SR inverted microscope and imaged with a Plan-Apochromat 63x / NA 1.4 oil immersion objective, with an additional 1.6x lens in the emission path. Images were captured with an Andor iXon 897 back-thinned EMCCD camera (16 bit, 512 x 512 pixels, 16 µm pixel size, QE 90%, set at -60°C working temperature), resulting in an image pixel size of 160 nm. Reference images in the green channel were taken with a 488 nm excitation laser (nominal output 300 mW) and a band pass (BP) 495-575 nm (+ LP 750) emission filter. For the far-red channel we used a 642 nm excitation laser (nominal output 150 mW) and a long pass (LP) 655 nm emission filter. SMLM recordings were performed exploiting the properties of the fluorescent protein mEos4 that is photoconverted from green to red state upon UV illumination (405 nm laser, nominal power 50 mW) and image acquisition in the red channel (561 nm laser, nominal power 200 mW, emission filter BP 570-650 + LP 750). The localisation precision of each detection was calculated from the fitting parameters and was obtained directly from the Zeiss NEO software. For the experiments reported here, the localisation precision was 33.1 ± 12.3 nm in x/y (mean ± SD).

Regarding the experiments in hippocampal cultures (data in Fig. 5), infected neurons expressing mEos4b-tagged GlyR subunits were identified in the green channel, and single reference epifluorescence images of 100 ms exposure were taken with the 488 nm excitation laser set at 1% and the 405 nm laser at 1% of the maximal power, and a camera gain of 100. For Sylite we used the far-red channel, taking one image of 100 ms with the 642 nm laser at 10% output and a camera gain of 10. A SMLM movie of 10000 frames was then recorded at 20 Hz streamed aquisition (50 ms frames) with constant 561 nm laser illumination at 100% laser output corresponding to a maximal power density of 0.95 kW/cm^2, and a gain 300. The photoconversion of mEos4b-tagged GlyR subunits (from green to red) was done by continuous 405 nm laser illumination that was gradually increased from 0.01 to 4% intensity (≤ 5.3 W/cm^2 irradiance).

For the detection of endogenous mEos4b-GlyRβ in brain slices (data in Fig. 1 and 3), we used the following acquisition parameters: Hippocampal and striatal regions were identified using NeuN immunolabelling in the green channel (AF488). A single epifluorescence image of 50 ms was taken with 488 nm illumation, 0.2% laser intensity, and a camera gain of 200 to record the NeuN immunofluorescence. Sylite was detected in the far-red channel, taking one image of 100 ms at 642 nm (5% output, camera gain 100). A first SMLM recording of 2000 frames at 20 Hz was done in the red channel with 561 nm laser illumination at 80% (irradiance 0.8 kW/cm^2), a camera gain of 300, and without 405 nm laser illumination. Under these conditions, mEos4b is not converted into the active (red) form. Afterwards, a second SMLM movie of 5000 frames was taken with the same settings, but with the addition of continuous 405 nm laser illumination that was gradually increased from 0.01 to 3% intensity (irradiance ≤ 4 W/cm^2). During these recordings, the total population of mEos4b molecules is converted (and bleached), since only very sparse detections are seen at the end of the movie. Glycinergic synapses in spinal cord slices (Supplementary Fig. S2) were identified as bright puncta of (unconverted) mEos4b-GlyRβ subunits in the green channel, and reference images were taken (green, mEos4b: 100 ms acquistion with the 488 laser at 0.2% power, camera gain 200; far-red, Sylite: 100 ms, 642 laser at 3%, gain 200 ms). SMLM movies of 15000 frames were recorded with the same settings as before with a continuous 405 nm laser illumination, gradually increasing from 0.01 to 5% intensity to ensure the complete conversion of mEos4b by the end of the experiment.

Epifluorescence image analysis in cultured neurons

For the analysis of cultured hippocampal neurons, only transduced cells expressing mEos4b-GlyRα1, α2 or β were considered (data in Fig. 5). Where the expression of the recombinant GlyR subunit was not obvious, this was confirmed by SMLM (Fig. 5B, see below) Within this population, the fraction of cells exhibiting synaptic localisation of GlyR was determined as the

number of cells in which mEos4b signals co-localised with Sylite-positive gephyrin clusters, as judged from the epifluorescence images (Fig. 5A). The fluorescence intensity of mEos4b-GlyRα1, α2 and β puncta at synapses was measured only in the infected neurons showing a synaptic localisation of the subunits. Synaptic puncta labelled with Sylite were detected using the spot detector plugin (Icy (de Chaumont et al., 2012)) with the following parameters: bright spots over dark background, detection scale 2 (sensitivity 40), and a size filter between 4 and 100 pixels. To restrict the analyses to synaptic puncta from infected neurons, the signal intensity in the mEos4b channel was thresholded using the mean + 2 SD calculated from uninfected control neurons. The pixel intensity was also corrected for the camera offset, by subtracting the minimum pixel intensity (1500 a.u.) from all images.

SMLM image analysis of mEos4b fluorescent protein

SMLM movies were processed with Zen software (Zeiss, Zen 2012 SP5 FP3 black, 64 bit) using a peak mask size of 7 pixels, a peak intensity of 6 and excluding the overlapping molecules. The single molecule localisations were corrected for x/y-drift with model-based algorithm (without fiducial markers). A rendered super-resolution image was reconstructed from the pointillist image, in which each detection is represented with a two-dimensional Gaussian distribution with a width corresponding to its point spread function (PSF) and a 10 nm pixel size and saved in tiff format.

Inhibitory synapses in spinal cord and brain slices were identified using the gephyrin-specific peptide marker Sylite (Khayenko et al., 2022). First, the Sylite reference images were adjusted to a 10 nm pixel size by multiplying the pixel number by a factor of 16. We then detected Sylite puncta using the spot detector plugin in Icy with these parameters: bright spots over dark background were detected at scale 5 set to a sensitivity of 100, and the size filtered between 400 and 10000 pixels. The obtained regions of interest (ROI) of Sylite were then employed as mask to measure the intensity of the mEos4b-GlyRβ signals in the rendered SMLM image. Where necessary, the alignment of the reference image and the rendered SMLM image were manually adjusted in ImageJ. To test the specificity of the co-localisation between Sylite and mEos4b-GlyRβ, we performed a pixel shift analysis with images of the CA3 region in $Glrb^{eos/eos}$ slices by horizontally flipping the Sylite channel relative to the mEos4b channel. The number of mEos4b-GlyRβ detections per gephyrin cluster was then recalculated using Icy software. The output data consist in an excel table containing the total intensity of Sylite and mEos4b-GlyRβ in each ROI. To convert the mEos4b-GlyRβ signals into detection numbers, the obtained total intensity values per ROI were divided by the integrated intensity of single mEos4b detections in the image.

A similar approach was used to estimate the copy numbers of mEos4b-GlyRβ containing GlyRs at inhibitory synapses in the CA3 region of the hippocampus. Rendered SMLM images of mEos4b-GlyRβ with a pixel size of 10 nm were segmented in Icy (detection of bright spots over dark background, scale 3 and 4 at a sensitivity of 100, and filtering between a size of 400–10000 pixels). Due to the low mEos4b-GlyRβ density in CA3, the obtained ROIs were considered to be clusters of detections arising from mEos4b fluorophores of a single heteropentameric GlyR (independent of its subunit stoichiometry). The average number of detections per cluster was then calculated by dividing the total intensity of the cluster by the total intensity of a single detection. This value was used as conversion factor to translate detection numbers into molecule numbers and was applied to all SMLM images from spinal cord, hippocampus and striatum. The copy numbers were further corrected by background subtraction using the negative control (CA3 region in wildtype C57BL/6J slices) and are given in Table 1.

Immunostaining of brain tissue slices used dual-colour SMLM with organic fluorophores

Frozen brain tissue from $Glrb^{eos/eos}$ mice (Maynard et al., 2021, Wiessler et al., 2024) was cut into 10 µm thick coronal cryostat sections and processed as described above. For dual-colour SMLM with organic fluorophores, the slices were labelled with primary antibodies against gephyrin (mAb7a mouse monoclonal, Synaptic Systems, #147011, 1:1000 dilution) and mEos

protein (AF647-conjugated FluoTag-X2, NanoTag Biotechnologies; #N3102-AF647-L, 1:500) overnight at 4°C, followed by secondary goat anti-mouse antibody coupled with a single CF680 dye (Biotium, #20817, 1:1000) for 4 h at RT. After washing in PBS, the slices were kept overnight at 4°C and imaged the next day.

Dual-colour SMLM acquisition and image processing

The cover glasses were placed in a closed Ludin chamber (Life Imaging Services) and, through the perfusion holes, was added a homemade dSTORM buffer (Yang & Specht, 2020) that was prepared as follows: A suspension containing 200 µg catalase (from bovine liver, Merck, # C30 1003493507) was washed three times with 1 ml of cold PBS and collected by centrifugation at 12000 g at 4°C for 1 min. After removing the supernatant, the catalase crystals were resuspended in 1 ml of PBS and incubated at 37°C with agitation for 30 min. The final dSTORM buffer was composed of PBS pH7.4, containing 50 mM cysteamine hydrochloride (= β-mercaptoethylamine, MEA, Merck, #M6500), 250 mM glucose (Merck, #G7021), 0.5 mg/ml glucose oxidase (from *Aspergillus niger*, Merck, #G2133-10KU) and 40 µg/ml dissolved catalase. Prior to use, the dSTORM buffer was degassed with N_2, transferred into a syringe and kept on ice.

SMLM experiments were carried with an Abbelight nanoscope (SAFe 360 Nexus SD) installed on the Zeiss Elyra PS1 setup described above, using two sCMOS cameras (Hamamatsu Orca-Fusion BT) for simultaneous dual-colour imaging. Before the acquisitions, the two cameras were aligned using 0.1 µm TetraSpeck beads (Invitrogen, #T-7279) deposited on a glass coverslip. The Ludin chamber with the tissue slices in dSTORM buffer was then placed on the stage of the inverted microscope and imaged with a Plan-Apochromat 100x / NA 1.46 oil-immersion objective without additional magnification. The far red AF647 and CF680 dyes were excited with a 640 nm laser of 520 mW nominal power (Oxxius LPX-640-500) using adaptable scanning of the excitation region (ASTER). SMLM images were acquired using NEOimaging software v.2.17.1 with the following parameters: 10000 images (image size 256 x 256 pixels and 97 nm pixel size) of 50 ms exposure were taken in the far-red channel with 80% laser power and a field of excitation set at 10%, resulting in a maximal irradiance of 20.3 kW/cm^2. Fluorophore blinking was gradually adjusted with a 405 nm laser (LBX-405-100, nominal output 108 mW), increasing the power from zero to 2% intensity along the recording (≤ 45 W/cm^2 irradiance). The emitted wavelengths were separated into two light paths with a 700 nm dichroic mirror for simultaneous dual-colour imaging and filtered with a band pass from 669 nm to 741 nm.

STORM images were processed with NEO analysis software (Abbelight v.39). The raw tiff movies from the transmitted camera (> 700 nm) and the reflected camera (< 700 nm) were loaded and processes sequentially. Single fluorophore signals were detected using temporal mean subtraction with a sliding window of 50 frames, and fit with a Gaussian distribution. The detection coordinates in both channels were corrected for x/y drift and saved as coordinate tables. For spectral demixing and image reconstruction (Supplementary Fig. S4), the detections from the two cameras were imported in the NEO 3D viewer, superimposed and automatically re-aligned. The intensity ratios for each detection were calculated according to the formula $I_{reflected}$ / ($I_{reflected}$ + $I_{transmitted}$), and we selected for each dye (AF647 and CF680) the inferior and superior cut-offs (0.25-0.32 for AF647); 0.42-0.70 for CF680). After removing the detections that had a precision ≥ 25 nm the spectrally demixed data were saved as coordinate tables and in the form of rendered super-resolution images with a normalized Gaussian representation of each detection and a pixel size of 10 nm. The mean localisation precision was calculated in NEO (Abbelight v.39) and was10.9 ± 4.4 (mean ± SD) for AF647 (anti-mEos nanobody) and 12.2 ± 4.9 for CF680 (anti-gephyrin).

The sub-synaptic distribution of GlyRs (AF647-labelled mEos4b-GlyRβ) and gephyrin (mAb7a-CF680) in hippocampal synapses in the CA3 region was investigated by DBSCAN cluster analysis implemented in NEO 3D viewer (Khayenko et al., 2022), using the following parameters: a radius of ε = 200 nm and n ≥ 5 neighbours for the AF647 detections (GlyRβ); and ε = 80 nm and n ≥ 50 neighbours for CF680 (gephyrin). We exported the data table containing the filtered clusters and their coordinates, and calculated the Euclidian distance between the centre of mass (CM) of the corresponding GlyR and gephyrin clusters, as well as the ratio of the GlyRβ-gephyrin distances

divided by the radius of gyration (RG) of the gephyrin cluster. Values <1 indicate that the GlyRβ detections are closer to the CM of gephyrin than the dispersion (RG) of the gephyrin detections themselves, suggesting that the GlyRs are integrated within the postsynaptic gephyrin cluster.

Confocal microscopy

For the control experiments shown in Fig. S3, spinal cord slices from *Glrb*$^{eos/eos}$ and wildtype animals (*Glrb*$^{WT/WT}$) were labelled with AF647-conjugated nanobody (1:1000, NanoTag) and with an antibody against gephyrin (mouse anti-gephyrin mAb7a, Synaptic Systems, 1:1000), followed by a donkey anti-mouse secondary antibody coupled with CF568 (Sigma #SAB4600075, 1:1000). Confocal images were taken on an SP8 microscope (Leica) using a 63x oil immersion objective and a Hybrid detector (HyD3). Acquisition of images (512 x 512 px, 16 bit) with a pixel size of 120 nm in the x/y plane and 1.27 µm in z (pinhole 1) was done in the three channels, green (mEos4b), red (CF568) and far-red (AF647).

Statistical analyses

Statistical analyses and graphing were performed using GraphPad Prism v.9. Data are represented as mean ± SD (standard deviation) or mean ± SEM (standard error of the mean) as indicated. Statistical significance was calculated using a non-parametric one-tailed or two-tailed Mann-Whitney test (MW), or a non-parametric Kruskal-Wallis test (KW, one-way ANOVA) with a post-hoc Dunn's multiple comparison test.

Preparation of acute brain slices

Adult C57BL/6J mice (postnatal day 35-41) were anesthetized with isoflurane and decapitated. The brains were quickly removed on ice and glued to the cooled stage of a vibratome (Leica VT 1200S). Coronal brain sections containing both dorsal and ventral striatum (150 µm) were sliced in ice-cold cutting solution (140 mM choline chloride, 26 mM $NaHCO_3$, 10 mM glucose, 7 mM $MgCl_2$, 2.5 mM KCl, 1.25 mM NaH_2PO_4, 0.5 mM $CaCl_2$, saturated with 95% O_2 and 5% CO_2). Brain slices were placed in recovery solution (120 mM NaCl, 2.5 mM KCl, 2 mM $CaCl_2$, 2 mM $MgCl_2$, 10 mM glucose, 26 mM $NaHCO_3$, 1.2 mM NaH_2PO_4, saturated with 95% O_2 and 5% CO_2) for 45 minutes at 32°C. Slices were kept at 32°C and used 1-4 h after slicing.

Electrophysiology

Acute brain slices were placed in the recording chamber and perfused with oxygenated aCSF (124 mM NaCl, 4.5 mM KCl, 2 mM $CaCl_2$, 10 mM glucose, 1 mM $MgCl_2$, 26 mM $NaHCO_3$, 1.2 mM NaH_2PO_4, saturated with 95% O_2 and 5% CO_2, pH 7.4, at room temperature). MSNs in the dorsal or ventral striatum were visualized using 4x air and 40x water immersion objectives of an upright Zeiss microscope (Axioskop 2FS Plus). A P-1000 micropipette puller (Sutter Instruments) was used to prepare filament-containing borosilicate glass patch pipettes (Hilgenberg GmbH) with a resistance of 4-5 MΩ. Patch pipettes were filled with internal solution (120 mM KCl, 4 mM $MgCl_2$, 10 mM HEPES, 1 mM EGTA, 5 mM Lidocaine N-ethyl bromide, 0.5 mM Na_2GTP, 2 mM Na_2ATP, adjusted to 280 mOsm, pH 7.4). Cells were recorded using voltage-clamp at a holding potential of -60 mV in whole cell configuration with a sampling rate of 10 kHz. During recordings, aCSF bath perfusion was applied for 1 minute. To pharmacologically isolate glycinergic mIPSCs, blockers of AMPA receptors (DNQX, 10 µM), nicotinic receptors (DHBE, 0.1 µM), NMDA receptors (L-689560, 5 µM), action potential firing (tetradotoxin, 0.5 µM) and $GABA_A$Rs (bicuculline, 10 µM) were added to aCSF and recorded for 5 minutes. To confirm that these mIPSCs were indeed glycinergic currents, strychnine was added at a concentration of 1 µM to the cocktail of blockers and recorded for an additional 1 minute. All recordings were acquired using a Multiclamp 700B amplifier (Axon Instruments), stored using 1440A Digidata (Axon Instruments), and analysed using Clampfit 10.7.0.3 (Axon Instruments) and NeuroExpress 24.c.16 (Szücs, 2022).

Acknowledgements

We thank Hans Maric (Virchow Center, University of Würzburg) for the Sylite probe, Carmen Villmann and Natascha Schäfer (Universitätsklinikum Würzburg) for the collection of brain and spinal cord tissue, Krishna Gaete Riquelme (Universidad de Concepción, Chile) for technical assistance, Nicolas Froger (MAPREG, France) for the supply of mouse embryos, Elisabeth Piccart and Petra Bex (UHasselt, Belgium) for brain slice patch clamp training, and Fabrice Schmitt (Zeiss) and Michael Schumacher (NeuroBicêtre, Inserm, UPSaclay) for their generous help with the setting up of the super-resolution imaging platform. We also acknowledge the proficient technical support by Zeiss and Abbelight.

Additional information

Data availability

The datasets generated for the current study are available from the corresponding author on reasonable request and will be deposited in a data repository upon article acceptance.

Author contributions

Experimentation: SC, YV

Data analysis: SC, YV, SYA

Experimental tools and techniques: CM, BB

Project design: SC, BB, CSP

Writing of the manuscript: SC, CSP

Editing of the manuscript: YV, SYA, BB

Funding acquisition: BB, CSP

Funding

This research was funded by the Agence Nationale de la Recherche (ANR-20-CE11-0002, InVivoNanoSpin, to CGS), Inserm (IRP RESiSTER, to CGS), and Fonds voor Wetenschappelijk Onderzoek (11N1422N, V419721N, to BB). SC was supported by a postdoctoral contract through the ANR projects InVivoNanoSpin (ANR-20-CE11-0002) and NeurATRIS (ANR-11-INBS-0011). The SMLM setup was acquired with the support of the Fédération pour la Recherche sur le Cerveau (FRC/Neurodon, opération Rotary – Espoir en Tête, to CGS), and an ERM equipment grant from UPSaclay (to CGS). We also acknowledge support of the international exchange programme ECOS Sud (C21S02, to CGS and Gonzalo Yévenes, UdeC, Chile).

Funding

Funder	Grant reference number	Author
Agence Nationale de la Recherche (ANR)	ANR-20-CE11-0002	Christian G Specht
Fonds Wetenschappelijk Onderzoek (FWO)	11N1422N	Bert Brône
Fonds Wetenschappelijk Onderzoek (FWO)	V419721N	Bert Brône
Institut National de la Santé et de la Recherche Médicale (Inserm)	IRP RESiSTER	Christian G Specht

Author ORCID iDs

Serena Camuso: http://orcid.org/0000-0002-3116-6340
Yana Vella: http://orcid.org/0000-0002-8592-1946

Bert Brône: http://orcid.org/0000-0002-4851-9480
Christian G Specht: http://orcid.org/0000-0001-6038-7735

Additional files

Supplemental information

References

Adermark L, Clarke RB, Ericson M, Söderpalm B (2011) Subregion-specific modulation of excitatory input and dopaminergic output in the striatum by tonically activated glycine and GABAa receptors. *Frontiers in systems neuroscience* **5**:85

Alvarez FJ (2017) Gephyrin and the regulation of synaptic strength and dynamics at glycinergic inhibitory synapses. *Brain Res Bull* **129**:50-65

Ceder MM, Magnusson KA, Weman HM, Henriksson K, Andréasson L, Lindström T, Wiggins O, Lagerström MC (2024) The mRNA expression profile of glycine receptor subunits alpha 1, alpha 2, alpha 4 and beta in female and male mice. *Mol Cell Neurosci* **131**:103976

Chapdelaine T, Hakim V, Triller A, Ranft J, Specht CG (2021) Reciprocal stabilization of glycine receptors and gephyrin scaffold proteins at inhibitory synapses. *Biophys J* **120**:805-817

Chattipakorn SC, McMahon LL (2002) Pharmacological characterization of glycine-gated chloride currents recorded in rat hippocampal slices. *J Neurophysiol* **87**:1515-25

Comhair J, Devoght J, Morelli G, Harvey RJ, Briz V, Borrie SC, Bagni C, Rigo J-M, Schiffmann SN, Gall D (2018) Alpha2-containing glycine receptors promote neonatal spontaneous activity of striatal medium spiny neurons and support maturation of glutamatergic inputs. *Frontiers in Molecular Neuroscience* **11**:380

Danglot L, Rostaing P, Triller A, Bessis A (2004) Morphologically identified glycinergic synapses in the hippocampus. *Mol Cell Neurosci* **27**:394-403

de Chaumont F, Dallongeville S, Chenouard N, Herve N, Pop S, Provoost T, Meas-Yedid V, Pankajakshan P, Lecomte T, Le Montagner Y, *et al.* (2012) Icy: an open bioimage informatics platform for extended reproducible research. *Nat Methods* **9**:690-6

Devoght J, Comhair J, Morelli G, Rigo JM, D'Hooge R, Touma C, Palme R, Dewachter I, vandeVen M, Harvey RJ, *et al.* (2023) Dopamine-mediated striatal activity and function is enhanced in GlyRα2 knockout animals. *iScience* **26**:107400

Durisic N, Godin AG, Wever CM, Heyes CD, Lakadamyali M, Dent JA (2012) Stoichiometry of the human glycine receptor revealed by direct subunit counting. *J Neurosci* **32**:12915-20

Durisic N, Laparra-Cuervo L, Sandoval-Alvarez A, Borbely JS, Lakadamyali M (2014) Single-molecule evaluation of fluorescent protein photoactivation efficiency using an in vivo nanotemplate. *Nat Methods* **11**:156-62

Fenech C, Winters BL, Otsu Y, Aubrey KR (2024) Supraspinal glycinergic neurotransmission in pain: A scoping review of current literature. *J Neurochem* **168**:3663-3684

Fujita M, Sato K, Sato M, Inoue T, Kozuka T, Tohyama M (1991) Regional distribution of the cells expressing glycine receptor beta subunit mRNA in the rat brain. *Brain Res* **560**:23-37

Grudzinska J, Schemm R, Haeger S, Nicke A, Schmalzing G, Betz H, Laube B (2005) The beta subunit determines the ligand binding properties of synaptic glycine receptors. *Neuron* **45**:727-39

Grunewald N, Jan A, Salvatico C, Kress V, Renner M, Triller A, Specht CG, Schwarz G (2018) Sequences flanking the gephyrin-binding site of GlyRbeta tune receptor stabilization at synapses. *eNeuro* **5**:ENEURO.0042-17.2018

Karlsson M, Zhang C, Méar L, Zhong W, Digre A, Katona B, Sjöstedt E, Butler L, Odeberg J, Dusart P, *et al.* (2021) A single-cell type transcriptomics map of human tissues. *Science advances* **7**

Kasaragod VB, Schindelin H (2018) Structure-function relationships of glycine and GABAA receptors and their interplay with the scaffolding protein gephyrin. *Front Mol Neurosci* **11**:317

Khayenko V, Schulte C, Reis SL, Avraham O, Schietroma C, Worschech R, Nordblom NF, Kachler S, Villmann C, Heinze KG, *et al.* (2022) A versatile synthetic affinity probe reveals inhibitory synapse ultrastructure and brain connectivity. *Angew Chem Int Ed Engl* **61**:e202202078

Kostrz D, Maynard SA, Schulte C, Laurent F, Masson J-B, Maric HM, Gosse C TRILLER A, Strick TR, Specht CG (2024) Competition between glycine and GABAA receptors for gephyrin controls their equilibrium populations at inhibitory synapses. *bioRxiv* https://doi.org/10.1101/2024.12.09.627587

Malosio ML, Marquèze-Pouey B, Kuhse J, Betz H (1991) Widespread expression of glycine receptor subunit mRNAs in the adult and developing rat brain. *Embo j* **10**:2401-9

Maric HM, Kasaragod VB, Hausrat TJ, Kneussel M, Tretter V, Stromgaard K, Schindelin H (2014) Molecular basis of the alternative recruitment of GABA(A) versus glycine receptors through gephyrin. *Nat Commun* **5**:5767

Maric HM, Mukherjee J, Tretter V, Moss SJ, Schindelin H (2011) Gephyrin-mediated gamma-aminobutyric acid type A and glycine receptor clustering relies on a common binding site. *J Biol Chem* **286**:42105-14

Maynard SA, Rostaing P, Schaefer N, Gemin O, Candat A, Dumoulin A, Villmann C, Triller A, Specht CG (2021) Identification of a stereotypic molecular arrangement of endogenous glycine receptors at spinal cord synapses. *eLife* **10**:e74441 https://doi.org/10.7554/eLife.74441

McCracken LM, Lowes DC, Salling MC, Carreau-Vollmer C, Odean NN, Blednov YA, Betz H, Harris RA, Harrison NL (2017) Glycine receptor α3 and α2 subunits mediate tonic and exogenous agonist-induced currents in forebrain. *Proc Natl Acad Sci U S A* **114**:E7179-e7186

Molander A, Söderpalm B (2005) Glycine receptors regulate dopamine release in the rat nucleus accumbens. *Alcohol Clin Exp Res* **29**:17-26

Molchanova SM, Comhair J, Karadurmus D, Piccart E, Harvey RJ, Rigo JM, Schiffmann SN, Brône B, Gall D (2017) Tonically active α2 subunit-containing glycine receptors regulate the excitability of striatal medium spiny neurons. *Front Mol Neurosci* **10**:442

Mori M, Gähwiler BH, Gerber U (2002) Beta-alanine and taurine as endogenous agonists at glycine receptors in rat hippocampus in vitro. *J Physiol* **539**:191-200

Muller E, Bakkar W, Martina M, Sokolovski A, Wong AY, Legendre P, Bergeron R (2013) Vesicular storage of glycine in glutamatergic terminals in mouse hippocampus. *Neuroscience* **242**:110-27

Muñoz B, Gallegos S, Peters C, Murath P, Lovinger DM, Homanics GE, Aguayo LG (2020) Influence of nonsynaptic α1 glycine receptors on ethanol consumption and place preference. *Addiction biology* **25**:e12726

Muñoz B, Yevenes GE, Förstera B, Lovinger DM, Aguayo LG (2018) Presence of inhibitory glycinergic transmission in medium spiny neurons in the nucleus accumbens. *Front Mol Neurosci* **11**:228

Notelaers K, Smisdom N, Rocha S, Janssen D, Meier JC, Rigo JM, Hofkens J, Ameloot M (2012) Ensemble and single particle fluorimetric techniques in concerted action to study the diffusion and aggregation of the glycine receptor alpha3 isoforms in the cell plasma membrane. *Biochim Biophys Acta* **1818**:3131-3140

Patrizio A, Renner M, Pizzarelli R, Triller A, Specht CG (2017) Alpha subunit-dependent glycine receptor clustering and regulation of synaptic receptor numbers. *Sci Rep* **7**:10899

Patrizio A, Specht CG (2016) Counting numbers of synaptic proteins: absolute quantification and single molecule imaging techniques. *Neurophotonics* **3**:041805

San Martin L, Gallegos S, Araya A, Romero N, Morelli G, Comhair J, Harvey RJ, Rigo JM, Brone B, Aguayo LG (2020) Ethanol consumption and sedation are altered in mice lacking the glycine receptor α2 subunit. *British Journal of Pharmacology* **177**:3941-3956

Song W, Chattipakorn SC, McMahon LL (2006) Glycine-gated chloride channels depress synaptic transmission in rat hippocampus. *J Neurophysiol* **95**:2366-79

Szücs A (2022) NeuroExpress program for analyzing patch-clamp data. *ResearchGate*

Weltzien F, Puller C, O'Sullivan GA, Paarmann I, Betz H (2012) Distribution of the glycine receptor beta-subunit in the mouse CNS as revealed by a novel monoclonal antibody. *J Comp Neurol* **520**:3962-81

Wiessler AL, Hasenmüller AS, Fuhl I, Mille C, Cortes Campo O, Reinhard N, Schenk J, Heinze KG, Schaefer N, Specht CG, *et al.* (2024) Role of the glycine receptor β subunit in synaptic localization and pathogenicity in severe startle disease. *J Neurosci* **44**

Wulffele J, Thédié D, Glushonkov O, Bourgeois D (2022) mEos4b Photoconversion Efficiency Depends on Laser Illumination Conditions Used in PALM. *The journal of physical chemistry letters* **13**:5075-5080

Yang X, Specht CG (2020) Practical guidelines for two-color SMLM of synaptic proteins in cultured neurons. In: Okada Y, Yamamoto N (Eds). *Single molecule microscopy in neurobiology* Springer. pp. 173-202

Yu H, Bai XC, Wang W (2021) Characterization of the subunit composition and structure of adult human glycine receptors. *Neuron* **109**:2707-2716.e6

Zeilhofer HU, Studler B, Arabadzisz D, Schweizer C, Ahmadi S, Layh B, Bosl MR, Fritschy JM (2005) Glycinergic neurons expressing enhanced green fluorescent protein in bacterial artificial chromosome transgenic mice. *J Comp Neurol* **482**:123-41

Zhu H, Gouaux E (2021) Architecture and assembly mechanism of native glycine receptors. *Nature* **599**:513-517

Peer reviews

Reviewer #1 (Public review):

Summary:

In this manuscript, the authors investigate the nanoscopic distribution of glycine receptor subunits in the hippocampus, dorsal striatum, and ventral striatum of the mouse brain using single-molecule localization microscopy (SMLM). They demonstrate that only a small number of glycine receptors are localized at hippocampal inhibitory synapses. Using dual-color SMLM, they further show that clusters of glycine receptors are predominantly localized within gephyrin-positive synapses. A comparison between the dorsal and ventral striatum reveals that the ventral striatum contains approximately eight times more glycine receptors and this finding is consistent with electrophysiological data on postsynaptic inhibitory currents. Finally, using cultured hippocampal neurons, they examine the differential synaptic localization of glycine receptor subunits (α1, α2, and β). This study is significant as it provides insights into the nanoscopic localization patterns of glycine receptors in brain regions where this protein is expressed at low levels. Additionally, the study demonstrates the different localization patterns of GlyR in distinct striatal regions and its physiological relevance using SMLM and electrophysiological experiments. However, several concerns should be addressed.

Specific comments on the original version:

(1) Colocalization analysis in Figure 1A. The colocalization between Sylite and mEos-GlyRβ appears to be quite low. It is essential to assess whether the observed colocalization is not due to random overlap. The authors should consider quantifying colocalization using statistical methods, such as a pixel shift analysis, to determine whether colocalization frequencies remain similar after artificially displacing one of the channels.

(2) Inconsistency between Figure 3A and 3B. While Figure 3B indicates an ~8-fold difference in the number of mEos4b-GlyRβ detections per synapse between the dorsal and ventral striatum, Figure 3A does not appear to show a pronounced difference in the localization of mEos4b-GlyRβ on Sylite puncta between these two regions. If the images presented in Figure

3A are not representative, the authors should consider replacing them with more representative examples or providing an expanded images with multiple representative examples. Alternatively, if this inconsistency can be explained by differences in spot density within clusters, the authors should explain that.

(3) Quantification in Figure 5. It is recommended that the authors provide quantitative data on cluster formation and colocalization with Sylite puncta in Figure 5 to support their qualitative observations.

(4) Potential for pseudo replication. It's not clear whether they're performing stats tests across biological replica, images, or even synapses. They often quote mean +/- SEM with n = 1000s, and so does that mean they're doing tests on those 1000s? Need to clarify.

(5) Does mEoS effect expression levels or function of the protein? Can't see any experiments done to confirm this. Could suggest WB on homogenate, or mass spec?

(6) Quantification of protein numbers is challenging with SMLM. Issues include i) some of FP not correctly folded/mature, and ii) dependence of localisation rate on instrument, excitation/illumination intensities, and also the thresholds used in analysis. Can the authors compare with another protein that has known expression levels- e.g. PSD95? This is quite an ask, but if they could show copy number of something known to compare with, it would be useful.

(7) Rationale for doing nanobody dSTORM not clear at all. They don't explain the reason for doing the dSTORM experiments. Why not just rely on PALM for coincidence measurements, rather than tagging mEoS with a nanobody, and then doing dSTORM with that? Can they explain? Is it to get extra localisations- i.e. multiple per nanobody? If so, localising same FP multiple times wouldn't improve resolution. Also, no controls for nanobody dSTORM experiments- what about non-spec nb, or use on WT sections?

(8) What resolutions/precisions were obtained in SMLM experiments? Should perform Fourier Ring Correlation (FRC) on SR images to state resolutions obtained (particularly useful for when they're presenting distance histograms, as this will be dependent on resolution). Likewise for precision, what was mean precision? Can they show histograms of localisation precision.

(9) Why were DBSCAN parameters selected? How can they rule out multiple localisations per fluor? If low copy numbers (<10), then why bother with DBSCAN? Could just measure distance to each one.

(10) For microscopy experiment methods, state power densities, not % or "nominal power".

(11) In general, not much data presented. Any SI file with extra images etc.?

(12) Clarification of the discussion on GlyR expression and synaptic localization: The discussion on GlyR expression, complex formation, and synaptic localization is sometimes unclear, and needs terminological distinctions between "expression level", "complex formation" and "synaptic localization". For example, the authors state: "What then is the reason for the low protein expression of GlyRβ? One possibility is that the assembly of mature heteropentameric GlyR complexes depends critically on the expression of endogenous GlyR α subunits." Does this mean that GlyRβ proteins that fail to form complexes with GlyRα subunits are unstable and subject to rapid degradation? If so, the authors should clarify this point. The statement "This raises the interesting possibility that synaptic GlyRs may depend specifically on the concomitant expression of both α1 and β transcripts." suggests a dependency on α1 and β transcripts. However, is the authors' focus on synaptic localization or overall protein expression levels? If this means synaptic localization, it would be beneficial to state this explicitly to avoid confusion. To improve clarity, the authors should

carefully distinguish between these different aspects of GlyR biology throughout the discussion. Additionally, a schematic diagram illustrating these processes would be highly beneficial for readers.

(13) Interpretation of GlyR localization in the context of nanodomains. The distribution of GlyR molecules on inhibitory synapses appears to be non-homogeneous, instead forming nanoclusters or nanodomains, similar to many other synaptic proteins. It is important to interpret GlyR localization in the context of nanodomain organization.

Significance:

The paper presents biological and technical advances. The biological insights revolve mostly on the documentation of Glycine receptors in particular synapses in forebrain, where they are typically expressed at very low levels. The authors provide compelling data indicating that the expression is of physiological significance. The authors have done a nice job of combining genetically tagged mice with advanced microscopy methods to tackle the question of distributions of synaptic proteins. Overall, these advances are more incremental than groundbreaking.

Comments on revised version:

The authors have addressed the majority of the significant issues raised in the review and revised the manuscript appropriately. One issue that can be further addressed relates to the issue of pseudo-replication. The authors state in their response that "All experiments were repeated at least twice to ensure reproducibility (N independent experiments). Statistical tests were performed on pooled data across the biological replicates; n denotes the number of data points used for testing (e.g., number of synaptic clusters, detections, cells, as specified in each case).". This suggests that they're not doing their stats on biological replicates, and instead are pseudo replicating. It's not clear how they have ensured reproducibility, when the stats seem to have been done on pooled data across repeats.

https://doi.org/10.7554/eLife.109447.1.sa3

Reviewer #2 (Public review):

Summary:

In their manuscript "Single molecule counting detects low-copy glycine receptors in hippocampal and striatal synapses" Camuso and colleagues apply single molecule localization microscopy (SMLM) methods to visualize low copy numbers of GlyRs at inhibitory synapses in the hippocampal formation and the striatum. SMLM analysis revealed higher copy numbers in striatum compared to hippocampal inhibitory synapses. They further provide evidence that these low copy numbers are tightly linked to post-synaptic scaffolding protein gephyrin at inhibitory synapses. Their approach profits from the high detection sensitivity and resolution of SMLM and challenges the controversial view on the presence of GlyRs in these formations although there are reports (electrophysiology) on the presence of GlyRs in these particular brain regions. These new datasets in the current manuscript may certainly assist in understanding the complexity of fundamental building blocks of inhibitory synapses.

Strengths:

The manuscript provides new insights to presence of low-copy numbers by visualizing them via SMLM. This is the first report that visualizes GlyR optically in the brain applying the knock-in model of mEOS4b tagged GlyRß and quantifies their copy number comparing distribution and amount of GlyRs from hippocampus and striatum. Imaging data correspond well to electrophysiological measurements in the manuscript.

Comments on revised version:

My concerns have been successfully addressed by the authors during the revision process.

https://doi.org/10.7554/eLife.109447.1.sa2

Reviewer #3 (Public review):

In this study, Camuso et al., make use of a knock-in mouse model expressing endogenously mEos4b-tagged GlyRβ subunits to detect endogenous glycine receptors in mouse brain using single-molecule localization microscopy (SMLM). At synapses in the hippocampus GlyRβ molecules are detected at very low copy numbers. Assuming that each detected GlyRβ molecule is incorporated in a pentameric glycine receptor, it was estimated that while the majority of hippocampal inhibitory synapses do not contain glycine receptors, a small population of inhibitory synapses contain a few (up to 10) glycine receptors. Using dual-color SMLM approaches it is furthermore confirmed that the detected GlyRβ molecules are embedded in the postsynaptic domain marked by gephyrin. In contrast to the hippocampus, at inhibitory synapses in the striatum GlyRβ molecules were detected at considerably higher copy numbers. Interestingly, the observed number of GlyRβ detections was significantly higher in the ventral striatum compared to the dorsal striatum. These findings are corroborated by electrophysiological recordings showing that postsynaptic glycinergic currents can be readily detected in the ventral striatum but are almost absent in the dorsal striatum. Using lentiviral overexpression of recombinant GlyRalpha1, alpha2, and beta subunits in cultured hippocampal neurons, it is shown that GlyR alpha1 subunits are readily detectable at synapses, but overexpressed GlyRalpha2 and beta subunits did not strongly enrich at synapses. This could indicate that GlyRa1 expression is limiting the synaptic expression of GlyRβ-containing glycine receptors in hippocampal neurons.

Comments on revised version:

This revised manuscript is significantly improved. New experimental and quantitative analysis is presented that strengthen the conclusions. Overall, the results presented in this manuscript are based on carefully performed SMLM experiments and are well-presented and described. The knock-in mouse with endogenously tagged GlyRβ molecules is a very strong aspect of this study and provides confidence in the labeling, the combination with SMLM is very strong as it provides high sensitivity and spatial resolution. These results confirm previous studies and will be of interest to a specialised audience interested in glycine receptors, inhibitory synapse biology and super-resolution microscopy.

https://doi.org/10.7554/eLife.109447.1.sa1

Author response:

The following is the authors' response to the current reviews.

We thank the editors of eLife and the reviewers for their thorough evaluation of our study. As regards the final comments of reviewer 1 please note that all experimental replicates were first analyzed separately, and were then pooled, since the observed changes were comparable between experiments. This mean that statistical analyses were done on pooled biological replicates.

The following is the authors' response to the original reviews.

General Statements

We thank the reviewers for their thorough and constructive evaluation of our work. We have revised the manuscript carefully and addressed all the criticisms raised, in particular the issues mentioned by several of the reviewers (see point-by-point response below). We have also added a number of explanations in the text for the sake of clarity, while trying to keep the manuscript as concise as possible.

In our view, the novelty of our research is two-fold. From a neurobiological point of view, we provide conclusive evidence for the existence of glycine receptors (GlyRs) at inhibitory synapses in various brain regions including the hippocampus, dentate gyrus and sub-regions of the striatum. This solves several open questions and has fundamental implications for our understanding of the organisation and function of inhibitory synapses in the telencephalon. Secondly, our study makes use of the unique sensitivity of single molecule localisation microscopy (SMLM) to identify low protein copy numbers. This is a new way to think about SMLM as it goes beyond a mere structural characterisation and towards a quantitative assessment of synaptic protein assemblies.

Point-by-point description of the revisions

> ***Reviewer #1 (Evidence, reproducibility and clarity):***
>
> *In this manuscript, the authors investigate the nanoscopic distribution of glycine receptor subunits in the hippocampus, dorsal striatum, and ventral striatum of the mouse brain using single-molecule localization microscopy (SMLM). They demonstrate that only a small number of glycine receptors are localized at hippocampal inhibitory synapses. Using dual-color SMLM, they further show that clusters of glycine receptors are predominantly localized within gephyrinpositive synapses. A comparison between the dorsal and ventral striatum reveals that the ventral striatum contains approximately eight times more glycine receptors and this finding is consistent with electrophysiological data on postsynaptic inhibitory currents. Finally, using cultured hippocampal neurons, they examine the differential synaptic localization of glycine receptor subunits (α1, α2, and β). This study is significant as it provides insights into the nanoscopic localization patterns of glycine receptors in brain regions where this protein is expressed at low levels. Additionally, the study demonstrates the different localization patterns of GlyR in distinct striatal regions and its physiological relevance using SMLM and electrophysiological experiments. However, several concerns should be addressed.*
>
> *The following are specific comments:*
>
> *(1) Colocalization analysis in Figure 1A. The colocalization between Sylite and mEos-GlyRβ appears to be quite low. It is essential to assess whether the observed colocalization is not due to random overlap. The authors should consider quantifying colocalization using statistical methods, such as a pixel shift analysis, to determine whether colocalization frequencies remain similar after artificially displacing one of the channels.*

Following the suggestion of reviewer 1, we re-analysed CA3 images of Glrb$^{eos/eos}$ hippocampal slices by applying a pixel-shift type of control, in which the Sylite channel (in far red) was horizontally flipped relative to the mEos4b-GlyRβ channel (in green, see Methods). As expected, the number of mEos4b-GlyRβ detections per gephyrin cluster was markedly reduced compared to the original analysis (revised Fig. 1B), confirming that the synaptic mEos4b detections exceed chance levels (see page 5).

> *(2) Inconsistency between Figure 3A and 3B. While Figure 3B indicates an ~8-fold difference in the number of mEos4b-GlyRβ detections per synapse between the dorsal and ventral striatum, Figure 3A does not appear to show a pronounced difference in the localization of mEos4bGlyRβ on Sylite puncta between these two regions. If the images presented in Figure 3A are not representative, the authors should consider replacing*

> *them with more representative examples or providing an expanded images with multiple representative examples. Alternatively, if this inconsistency can be explained by differences in spot density within clusters, the authors should explain that.*

The pointillist images in Fig. 3A are essentially binary (red-black). Therefore, the density of detections at synapses cannot be easily judged by eye. For clarity, the original images in Fig. 3A have been replaced with two other examples that better reflect the different detection numbers in the dorsal and ventral striatum.

> *(3) Quantification in Figure 5. It is recommended that the authors provide quantitative data on cluster formation and colocalization with Sylite puncta in Figure 5 to support their qualitative observations.*

This is an important point that was also raised by the other reviewers. We have performed additional experiments to increase the data volume for analysis. For quantification, we used two approaches. First, we counted the percentage of infected cells in which synaptic localisation of the recombinant receptor subunit was observed (Fig. 5C). We found that mEos4b-GlyRa1 consistently localises at synapses, indicating that all cells express endogenous GlyRb. When neurons were infected with mEos4b-GlyRb, fewer cells had synaptic clusters, meaning that indeed, GlyR alpha subunits are the limiting factor for synaptic targeting. In cultures infected with mEos4b-GlyRa2, only very few neurons displayed synaptic localisation (as judged by epifluorescence imaging). We think this shows that GlyRa2 is less capable of forming heteromeric complexes than GlyRa1, in line with our previous interpretation (see pp. 9-10, 13).

Secondly, we quantified the total intensity of each subunit at gephyrin-positive domains, both in infected neurons as well as non-infected control cultures (Fig. 5D). We observed that mEos4bGlyRa1 intensity at gephyrin puncta was higher than that of the other subunits, again pointing to efficient synaptic targeting of GlyRa1. Gephyrin cluster intensities (Sylite labelling) were not significantly different in GlyRb and GlyRa2 expressing neurons compared to the uninfected control, indicating that the lentiviral expression of recombinant subunits does not fundamentally alter the size of mixed inhibitory synapses in hippocampal neurons. Interestingly, gephyrin levels were slightly higher in hippocampal neurons expressing mEos4b-GlyRa1. In our view, this comes from an enhanced expression and synaptic targeting of mEos4b-GlyRa1 heteromers with endogenous GlyRb, pointing to a structural role of GlyRa1/b in hippocampal synapses (pp. 10, 13).

The new data and analyses have been described and illustrated in the relevant sections of the manuscript.

> *(4) Potential for pseudo replication. It's not clear whether they're performing stats tests across biological replica, images, or even synapses. They often quote mean +/- SEM with n = 1000s, and so does that mean they're doing tests on those 1000s? Need to clarify.*

All experiments were repeated at least twice to ensure reproducibility (N independent experiments). Statistical tests were performed on pooled data across the biological replicates; n denotes the number of data points used for testing (e.g., number of synaptic clusters, detections, cells, as specified in each case). We have systematically given these numbers in the revised manuscript (n, N, and other experimental parameters such as the number of animals used, coverslips, images or cells). Data are generally given as mean +/- SEM or as mean +/- SD as indicated.

> *(5) Does mEoS effect expression levels or function of the protein? Can't see any experiments done to confirm this. Could suggest WB on homogenate, or mass spec?*

The $Glrb^{eos/eos}$ knock-in mouse line has been characterised previously and does not to display any ultrastructural or functional deficits at inhibitory synapses (Maynard et al. 2021 eLife).

GlyRβ expression and glycine-evoked responses were not significantly different to those of the wildtype. The synaptic localisation of mEos4b-GlyRb in KI animals demonstrates correct assembly of heteromeric GlyRs and synaptic targeting. Accordingly, the animals do not display any obvious phenotype. We have clarified this in the manuscript (p. 4). In the case of cultured neurons, long-term expression of fluorescent receptor subunits with lentivirus has proven ideal to achieve efficient synaptic targeting. The low and continuous supply of recombinant receptors ensures assembly with endogenous subunits to form heteropentameric receptor complexes (e.g. [Patrizio et al. 2017 Sci Rep]). In the present study, lentivirus infection did not induce any obvious differences in the number or size of inhibitory synapses compared to control neurons, as judged by Sylite labelling of synaptic gephyrin puncta (new Fig. 5D).

> *(6) Quantification of protein numbers is challenging with SMLM. Issues include i) some of FP not correctly folded/mature, and ii) dependence of localisation rate on instrument, excitation/illumination intensities, and also the thresholds used in analysis. Can the authors compare with another protein that has known expression levels- e.g. PSD95? This is quite an ask, but if they could show copy number of something known to compare with, it would be useful.*

We agree that absolute quantification with SMLM is challenging, since the number of detections depends on fluorophore maturation, photophysics, imaging conditions, and analysis thresholds (discussed in Patrizio & Specht 2016, Neurophotonics). For this reason, only very few datasets provide reliable copy numbers, even for well-studied proteins such as PSD-95. One notable exception is the study by Maynard et al. (eLife 2021) that quantified endogenous GlyRβcontaining receptors in spinal cord synapses using SMLM combined with correlative electron microscopy. The strength of this work was the use of a KI mouse strain, which ensures that mEos4b-GlyRβ expression follows intrinsic regional and temporal profiles. The authors reported a stereotypic density of ~2,000 GlyRs/µm² at synapses, corresponding to ~120 receptors per synapse in the dorsal horn and ~240 in the ventral horn, taking into account various parameters including receptor stoichiometry and the functionality of the fluorophore. These values are very close to our own calculations of GlyR numbers at spinal cord synapses that were obtained slightly differently in terms of sample preparation, microscope setup, imaging conditions, and data analysis, lending support to our experimental approach. Nevertheless, the obtained GlyR copy numbers at hippocampal synapses clearly have to be taken as estimates rather than precise figures, because the number of detections from a single mEos4b fluorophore can vary substantially, meaning that the fluorophores are not represented equally in pointillist images. This can affect the copy number calculation for a specific synapse, in particular when the numbers are low (e.g. in hippocampus), however, it should not alter the average number of detections (Fig. 1B) or the (median) molecule numbers of the entire population of synapses (Fig. 1C). We have discussed the limitations of our approach (p. 11).

> *(7) Rationale for doing nanobody dSTORM not clear at all. They don't explain the reason for doing the dSTORM experiments. Why not just rely on PALM for coincidence measurements, rather than tagging mEoS with a nanobody, and then doing dSTORM with that? Can they explain? Is it to get extra localisations- i.e. multiple per nanobody? If so, localising same FP multiple times wouldn't improve resolution. Also, no controls for nanobody dSTORM experiments- what about non-spec nb, or use on WT sections?*

As discussed above (point 6), the detection of fluorophores with SMLM is influenced by many parameters, not least the noise produced by emitting molecules other than the fluorophore used for labelling. Our study is exceptional in that it attempts to identify extremely low molecule numbers (down to 1). To verify that the detections obtained with PALM correspond to mEos4b, we conducted robust control experiments (including pixel-shift as suggested by the reviewer, see point 1, revised Fig. 1B). The rationale for the nanobody-based dSTORM

experiments was twofold: (1) to have an independent readout of the presence of low-copy GlyRs at inhibitory synapses and (2) to analyse the nanoscale organisation of GlyRs relative to the synaptic gephyrin scaffold using dual-colour dSTORM with spectral demixing (see p. 6). The organic fluorophores used in dSTORM (AF647, CF680) ensure high photon counts, essential for reliable co-localisation and distance analysis. PALM and dSTORM cannot be combined in dual-colour mode, as they require different buffers and imaging conditions.

The specificity of the anti-Eos nanobody was demonstrated by immunohistochemistry in spinal cord cultures expressing mEos4b-GlyRb and wildtype control tissue (Fig. S3). In response to the reviewer's remarks, we also performed a negative control experiment in $Glrb^{eos/eos}$ slices (dSTORM), in which the nanobody was omitted (new Fig. S4F,G). Under these conditions, spectral demixing produced a single peak corresponding to CF680 (gephyrin) without any AF647 contribution (Fig. S4F). The background detection of "false" AF647 detections at synapses was significantly lower than in the slices labelled with the nanobody. We conclude that the fluorescence signal observed in our dual-colour dSTORM experiments arises from the specific detection of mEos4b-GlyRb by the nanobody, rather than from background, crossreactivity or wrong attribution of colour during spectral demixing. We have added these data and explanations in the results (p. 7) and in the figure legend of Fig. S4F,G.

> *(8) What resolutions/precisions were obtained in SMLM experiments? Should perform Fourier Ring Correlation (FRC) on SR images to state resolutions obtained (particularly useful for when they're presenting distance histograms, as this will be dependent on resolution). Likewise for precision, what was mean precision? Can they show histograms of localisation precision.*

This is an interesting question in the context of our experiments with low-copy GlyRs, since the spatial resolution of SMLM is limited also by the density of molecules, i.e. the sampling of the structure in question (Nyquist-Shannon criterion). Accordingly, the priority of the PALM experiments was to improve the sensibility of SMLM for the identification of mEos4b-GlyRb subunits, rather than to maximize the spatial resolution. The mean localisation precision in PALM was 33 +/- 12 nm, as calculated from the fitting parameters of each detection (Zeiss, ZEN software), which ultimately result from their signal-to-noise ratio. This is a relatively low precision for SMLM, which can be explained by the low brightness of mEos4b compared to organic fluorophores together with the elevated fluorescence background in tissue slices.

In the case of dSTORM, the aim was to study the relative distribution of GlyRs within the synaptic scaffold, for which a higher localisation precision was required (p. 6). Therefore, detections with a precision ≥ 25 nm were filtered during analysis with NEO software (Abbelight). The retained detections had a mean localisation precision of 12 +/- 5 for CF680 (Sylite) and 11 +/- 4 for AF647 (nanobody). These values are given in the revised manuscript (pp. 18, 22).

> *(9) Why were DBSCAN parameters selected? How can they rule out multiple localisations per fluor? If low copy numbers (<10), then why bother with DBSCAN? Could just measure distance to each one.*

Multiple detections of the same fluorophore are intrinsic to dSTORM imaging and have not been eliminated from the analysis. Small clusters of detections likely represent individual molecules (e.g. single receptors in the extrasynaptic regions, Fig. 2A). DBSCAN is a robust clustering method that is quite insensitive to minor changes in the choice of parameters. For dSTORM of synaptic gephyrin clusters (CF680), a relatively low length (80 nm radius) together with a high number of detections (≥ 50 neighbours) were chosen to reconstruct the postsynaptic domain with high spatial resolution (see point 8). In the case of the GlyR (nanobody-AF647), the clustering was done mostly for practical reasons, as it provided the coordinates of the centre of mass of the detections. The low stringency of this clustering (200

nm radius, ≥ 5 neighbours) effectively filters single detections that can result from background noise or incorrect demixing. An additional reference explaining the use of DBSCAN including the choice of parameters is given on p. 22 (see also R2 point 4).

> *(10) For microscopy experiment methods, state power densities, not % or "nominal power".*

Done. We now report the irradiance (laser power density) instead of nominal power (pp. 18, 21).

> *(11) In general, not much data presented. Any SI file with extra images etc.?*

The original submission included four supplementary figures with additional data and representative images that should have been available to the reviewer (Figs. S1-S4). The SI file has been updated during revision (new Fig. S4E-G).

> *(12) Clarification of the discussion on GlyR expression and synaptic localization: The discussion on GlyR expression, complex formation, and synaptic localization is sometimes unclear, and needs terminological distinctions between "expression level", "complex formation" and "synaptic localization". For example, the authors state:"What then is the reason for the low protein expression of GlyRβ? One possibility is that the assembly of mature heteropentameric GlyR complexes depends critically on the expression of endogenous GlyR α subunits." Does this mean that GlyRβ proteins that fail to form complexes with GlyRα subunits are unstable and subject to rapid degradation? If so, the authors should clarify this point. The statement "This raises the interesting possibility that synaptic GlyRs may depend specifically on the concomitant expression of both α1 and β transcripts." suggests a dependency on α1 and β transcripts. However, is the authors' focus on synaptic localization or overall protein expression levels? If this means synaptic localization, it would be beneficial to state this explicitly to avoid confusion. To improve clarity, the authors should carefully distinguish between these different aspects of GlyR biology throughout the discussion. Additionally, a schematic diagram illustrating these processes would be highly beneficial for readers.*

We thank the reviewer to point this out. We are dealing with several processes; protein expression that determines subunit availability and the assembly of pentameric GlyRs complexes, surface expression, membrane diffusion and accumulation of GlyRb-containing receptor complexes at inhibitory synapses. We have edited the manuscript, particularly the discussion and tried to be as clear as possible in our wording.

We chose not to add a schematic illustration for the time being, because any graphical representation is necessarily a simplification. Instead, we preferred to summarise the main numbers in tabular form (Table 1). We are of course open to any other suggestions.

> *(13) Interpretation of GlyR localization in the context of nanodomains. The distribution of GlyR molecules on inhibitory synapses appears to be non-homogeneous, instead forming nanoclusters or nanodomains, similar to many other synaptic proteins. It is important to interpret GlyR localization in the context of nanodomain organization.*

The dSTORM images in Fig. 2 are pointillist representations that show individual detections rather than molecules. Small clusters of detections are likely to originate from a single AF647 fluorophore (in the case of nanobody labelling) and therefore represent single GlyRb subunits. Since GlyR copy numbers are so low at hippocampal synapses (≤ 5), the notion of nanodomain is not directly applicable. Our analysis therefore focused on the integration of GlyRs within the postsynaptic scaffold, rather than attempting to define nanodomain structures (see also response to point 8 of R1). A clarification has been added in the revised manuscript (p. 6).

> *The paper presents biological and technical advances. The biological insights revolve mostly on the documentation of Glycine receptors in particular synapses in forebrain, where they are typically expressed at very low levels. The authors provide compelling data indicating that the expression is of physiological significance. The authors have done a nice job of combining genetically-tagged mice with advanced microscopy methods to tackle the question of distributions of synaptic proteins. Overall these advances are more incremental than groundbreaking.*

We thank the reviewer for acknowledging both the technical and biological advances of our study. While we recognize that our work builds upon established models, we consider that it also addresses important unresolved questions, namely that GlyRs are present and specifically anchored at inhibitory synapses in telencephalic regions, such as the hippocampus and striatum. From a methodological point of view, our study demonstrates that SMLM can be applied not only for structural analysis of highly abundant proteins, but also to reliably detect proteins present at very low copy numbers. This ability to identify and quantify sparse molecule populations adds a new dimension to SMLM applications, which we believe increases the overall impact of our study beyond the field of synaptic neuroscience.

> ***Reviewer #2 (Evidence, reproducibility and clarity):***
>
> *In their manuscript "Single molecule counting detects low-copy glycine receptors in hippocampal and striatal synapses" Camuso and colleagues apply single molecule localization microscopy (SMLM) methods to visualize low copy numbers of GlyRs at inhibitory synapses in the hippocampal formation and the striatum. SMLM analysis revealed higher copy numbers in striatum compared to hippocampal inhibitory synapses. They further provide evidence that these low copy numbers are tightly linked to post-synaptic scaffolding protein gephyrin at inhibitory synapses. Their approach profits from the high sensitivity and resolution of SMLM and challenges the controversial view on the presence of GlyRs in these formations although there are reports (electrophysiology) on the presence of GlyRs in these particular brain regions. These new datasets in the current manuscript may certainly assist in understanding the complexity of fundamental building blocks of inhibitory synapses.*
>
> *However I have some minor points that the authors may address for clarification:*
>
> *(1) In Figure 1 the authors apply PALM imaging of mEos4b-GlyRß (knockin) and here the corresponding Sylite label seems to be recorded in widefield, it is not clearly stated in the figure legend if it is widefield or super-resolved. In Fig 1 A - is the scale bar 5 µm? Some Sylite spots appear to be sized around 1 µm, especially the brighter spots, but maybe this is due to the lower resolution of widefield imaging? Regarding the statistical comparison: what method was chosen to test for normality distribution, I think this point is missing in the methods section.*

This is correct; the apparent size of the Sylite spots does not reflect the real size of the synaptic gephyrin domain due to the limited resolution of widefield imaging including the detection of outof-focus light. We have clarified in the legend of Fig. 1A that Sylite labelling was with classic epifluorescence microscopy. The scale bar in Fig. 1A corresponds to 5 µm. Since the data were not normally distributed, nonparametric tests (Kruskal- Wallis one-way ANOVA with Dunn's multiple comparison test or Mann-Whitney U-test for pairwise comparisons) were used (p. 23).

Moreover I would appreciate a clarification and/or citation that the knockin model results in no structural and physiological changes at inhibitory synapses, I believe this model has been applied in previous studies and corresponding clarification can be provided.

The Glrbeos/eos mouse model has been described previously and does not exhibit any structural or physiological phenotypes (Maynard et al. 2021 eLife). The issue was also raised by reviewer R1 (point 5) and has been clarified in the revised manuscript (p. 4).

> *(2) In the next set of experiments the authors switch to demixing dSTORM experiments - an explanation why this is performed is missing in the text - I guess better resolution to perform more detailed distance measurements? For these experiments: which region of the hippocampus did the authors select, I cannot find this information in legend or main text.*

Yes, the dSTORM experiments enable dual-colour structural analysis at high spatial resolution (see response to R1 point 7). An explanation has been added (p. 6).

> *(3) Regarding parameters of demixing experiments: the number of frames (10.000) seems quite low and the exposure time higher than expected for Alexa 647. Can the authors explain the reason for chosing these particular parameters (low expression profile of the target - so better separation?, less fluorophores on label and shorter collection time?) or is there a reference that can be cited? The laser power is given in the methods in percentage of maximal output power, but for better comparison and reproducibility I recommend to provide the values of a power meter (kW/cm2) as lasers may change their maximum output power during their lifetime.*

Acquisition parameters (laser power, exposure time) for dSTORM were chosen to obtain a good localisation precision (~12 nm; see R1 point 8). The number of frames is adequate to obtain well sampled gephyrin scaffolds in the CF680 channel. In the case of the GlyR (nanobody-AF647), the concept of spatial resolution does not really apply due to the low number of targets (see R1, point 13). Power density (irradiance) values have now been given (pp. 18, 21).

> *(4) For analysis of subsynaptic distribution: how did the authors decide to choose the parameters in the NEO software for DBSCAN clustering - was a series of parameters tested to find optimal conditions and did the analysis start with an initial test if data is indeed clustered (K-ripley) or is there a reference in literature that can be provided?*

DBSCAN parameters were optimised manually, by testing different values. Identification of dense and well-delimited gephyrin clusters (CF680) was achieved with a small radius and a high number of detections (80 nm, ≥ 50 neighbours), whereas filtering of low-density background in the AF647 channel (GlyRs) required less stringent parameters (200 nm, ≥ 5) due to the low number of target molecules. Similar parameters were used in a previous publication (Khayenko et al. 2022, Angewandte Chemie). The reference has been provided on p. 22 (see also R1 point 9).

> *(5) A conclusion/discussion of the results presented in Figure 5 is missing in the text/discussion.*

This part of the manuscript has been completely overhauled. It includes new experimental data, quantification of the data (new Fig.5), as well as the discussion and interpretation of our findings (see also R1, point 3). In agreement with our earlier interpretation, the data confirm that low availability of GlyRa1 subunits limits the expression and synaptic targeting of GlyRa1/b heteropentamers. The observation that GlyRa1 overexpression with lentivirus increases the size of the postsynaptic gephyrin domain further points to a structural role, whereby GlyRs can enhance the stability (and size) of inhibitory synapses in hippocampal neurons, even at low copy numbers (pp. 13-14).

> *(6) In line 552 "suspension" is misleading, better use "solution"*

Done.

> ***Reviewer #2 (Significance):***
>
> *Significance: The manuscript provides new insights to presence of low-copy numbers by visualizing them via SMLM. This is the first report that visualizes GlyR optically in the brain applying the knock-in model of mEOS4b tagged GlyRß and quantifies their copy number comparing distribution and amount of GlyRs from hippocampus and striatum. Imaging data correspond well to electrophysiological measurements in the manuscript.*
>
> *Field of expertise: Super-Resolution Imaging and corresponding analysis*
>
> ***Reviewer #4 (Evidence, reproducibility and clarity):***
>
> *In this study, Camuso et al., make use of a knock-in mouse model expressing endogenously mEos4b-tagged GlyRβ to detect endogenous glycine receptors using single-molecule localization microscopy. The main conclusion from this study is that in the hippocampus GlyRβ molecules are barely detected, while inhibitory synapses in the ventral striatum seem to express functionally relevant GlyR numbers.*
>
> *I have a few points that I hope help to improve the strength of this study.*
>
> *- In the hippocampus, this study finds that the numbers of detections are very low. The authors perform adequate controls to indicate that these localizations are above noise level. Nevertheless, it remains questionable that these reflect proper GlyRs. The suggestion that in hippocampal synapses the low numbers of GlyRβ molecules "are important in assembly or maintenance of inhibitory synaptic structures in the brain" is on itself interesting, but is not at all supported. It is also difficult to envision how such low numbers could support the structure of a synapse. A functional experiment showing that knockdown of GlyRs affects inhibitory synapse structure in hippocampal neurons would be a minimal test of this.*

It is not clear what the reviewer means by “it remains questionable that these reflect proper GlyRs”. The PALM experiments include a series of stringent controls (see R1, point 1) demonstrating the existence of low-copy GlyRs at inhibitory synapses in the hippocampus (Fig. 1) and in the striatum (Fig. 3), and are backed up by dSTORM experiments (Fig. 2). We have no reason to doubt that these receptors are fully functional (as demonstrated for the ventral striatum (Fig. 4). However, due to their low number, a role in inhibitory synaptic transmission is clearly limited, at least in the hippocampus and dorsal striatum.

We therefore propose a structural role, where the GlyRs could be required to stabilise the postsynaptic gephyrin domain in hippocampal neurons. This is based on the idea that the GlyRgephyrin affinity is much higher than that of the GABAAR-gephyrin interaction (reviewed in Kasaragod & Schindelin 2018 Front Mol Neurosci). Accordingly, there is a close relationship between GlyRs and gephyrin numbers, sub-synaptic distribution, and dynamics in spinal cord synapses that are mostly glycinergic (Specht et al. 2013 Neuron; Maynard et al. 2021 eLife; Chapdelaine et al. 2021 Biophys J). It is reasonable to assume that low-copy GlyRs could play a similar structural role at hippocampal synapses. A knockdown experiment targeting these few receptors is technically very challenging and beyond the scope of this study. However, in response to the reviewer's question we have conducted new experiments in cultured hippocampal neurons (new Fig. 5). They demonstrate that overexpression of GlyRa1/b heteropentamers increases the size of the postsynaptic domain in these neurons, supporting our interpretation of a structural role of low-copy GlyRs (p. 14).

> *- The endogenous tagging strategy is a very strong aspect of this study and provides confidence in the labeling of GlyRβ molecules. One caveat however, is that this labeling*

> *strategy does not discriminate whether GlyRβ molecules are on the cell membrane or in internal compartments. Can the authors provide an estimate of the ratio of surface to internal GlyRβ molecules?*

Gephyrin is known to form a two-dimensional scaffold below the synaptic membrane to which inhibitory GlyRs and GABAARs attach (reviewed in Alvarez 2017 Brain Res). The majority of the synaptic receptors are therefore thought to be located in the synaptic membrane, which is supported by the close relationship between the sub-synaptic distribution of GlyRs and gephyrin in spinal cord neurons (e.g. Maynard et al. 2021 eLife). To demonstrate the surface expression of GlyRs at hippocampal synapses we labelled cultured hippocampal neurons expressing mEos4b-GlyRa1 with anti-Eos nanobody in non-permeabilised neurons (see Author response image 1). The close correspondence between the nanobody (AF647) and the mEos4b signal confirms that the majority of the GlyRs are indeed located in the synaptic membrane.

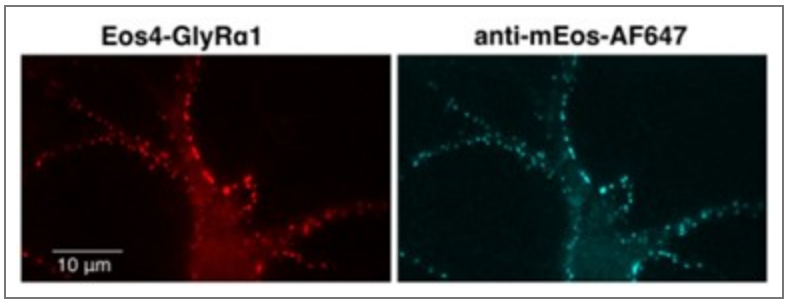

Author response image 1. Left: Lentivirus expression of mEos4b-GlyRa1 in fixed and non-permeabilised hippocampal neurons (mEos4b signal). Right: Surface labelling of the recombinant subunit with anti-Eos nanoboby (AF647).

> *- "We also estimated the absolute number of GlyRs per synapse in the hippocampus. The number of mEos4b detections was converted into copy numbers by dividing the detections at synapses by the average number of detections of individual mEos4b-GlyRβ containing receptor complexes". In essence this is a correct method to estimate copy numbers, and the authors discuss some of the pitfalls associated with this approach (i.e., maturation of fluorophore and detection limit). Nevertheless, the authors did not subtract the number of background localizations determined in the two negative control groups. This is critical, particularly at these low-number estimations.*

We fully agree that background subtraction can be useful with low detection numbers. In the revised manuscript, copy numbers are now reported as background-corrected values. Specifically, the mean number of detections measured in wildtype slices was used to calculate an equivalent receptor number, which was then subtracted from the copy number estimates across hippocampus, spinal cord and striatum. This procedure is described in the methods (p. 20) and results (p. 5, 8), and mentioned in the figure legends of Fig. 1C, 3C. The background corrected values are given in the text and Table 1.

> *- Furthermore, the authors state that "The advantage of this estimation is that it is independent of the stoichiometry of heteropentameric GlyRs". However, if the stoichometry is unknown, the number of counted GlyRβ subunits cannot simply be reported as the number of GlyRs. This should be discussed in more detail, and more carefully reported throughout the manuscript.*

The reviewer is right to point this out. There is still some debate about the stoichiometry of heteropentameric GlyRs. Configurations with 2a:3b, 3a:2b and 4a:1b subunits have been advanced (e.g. Grudzinska et al. 2005 Neuron; Durisic et al. 2012 J Neurosci; Patrizio et al.

2017 Sci Rep; Zhu & Gouaux 2021 Nature). We have therefore chosen a quantification that is independent of the underlying stoichiometry. Since our quantification is based on very sparse clusters of mEos4b detections that likely originate from a single receptor complex (irrespective of its stoichiometry), the reported values actually reflect the number of GlyRs (and not GlyRb subunits). We have clarified this in the results (p. 5) and throughout the manuscript (Table 1).

> *- The dual-color imaging provides insights in the subsynaptic distribution of GlyRβ molecules in hippocampal synapses. Why are similar studies not performed on synapses in the ventral striatum where functionally relevant numbers of GlyRβ molecules are found? Here insights in the subsynaptic receptor distribution would be of much more interest as it can be tight to the function.*

This is an interesting suggestion. However, the primary aim of our study was to identify the existence of GlyRs in hippocampal regions. At low copy numbers, the concept of sub-synaptic domains (SSDs, e.g. Yang et al. 2021 EMBO Rep) becomes irrelevant (see R1 point 13). It should be pointed out that the dSTORM pointillist images (Fig. 2A) represent individual GlyR detections rather than clusters of molecules. In the striatum, our specific purpose was to solve an open question about the presence of GlyRs in different subregions (putamen, nucleus accumbens).

> *- It is unclear how the experiments in Figure 5 add to this study. These results are valid, but do not seem to directly test the hypothesis that "the expression of α subunits may be limiting factor controlling the number of synaptic GlyRs". These experiments simply test if overexpressed α subunits can be detected. If the α subunits are limiting, measuring the effect of α subunit overexpression on GlyRβ surface expression would be a more direct test.*

Both R1 and R2 have also commented on the data in Fig. 5 and their interpretation. We have substantially revised this section as described before (see R1 point 3) including additional experiments and quantification of the data (new Fig. 5). The findings lend support to our earlier hypothesis that GlyR alpha subunits (in particular GlyRa1) are the limiting factor for the expression of heteropentameric GlyRa/b in hippocampal neurons (pp. 13-14). Since the GlyRa1 subunit itself does not bind to gephyrin (Patrizio et al. 2017 Sci Rep), the synaptic localisation of the recombinant mEos4b-GlyRa1 subunits is proof that they have formed heteropentamers with endogenous GlyRb subunits and driven their membrane trafficking, which the GlyRb subunits are incapable of doing on their own.

> ***Reviewer #4 (Significance):***
>
> *These results are based on carefully performed single-molecule localization experiments, and are well-presented and described. The knockin mouse with endogenously tagged GlyRβ molecules is a very strong aspect of this study and provides confidence in the labeling, the combination with single-molecule localization microscopy is very strong as it provides high sensitivity and spatial resolution.*
>
> *The conceptual innovation however seems relatively modest, these results confirm previous studies but do not seem to add novel insights. This study is entirely descriptive and does not bring new mechanistic insights.*
>
> *This study could be of interest to a specialized audience interested in glycine receptor biology, inhibitory synapse biology and super-resolution microscopy.*
>
> *My expertise is in super-resolution microscopy, synaptic transmission and plasticity*

As we have stated before, the novelty of our study lies in the use of SMLM for the identification of very small numbers of molecules, which requires careful control

experiments. This is something that has not been done before and that can be of interest to a wider readership, as it opens up SMLM for ultrasensitive detection of rare molecular events. Using this approach, we solve two open scientific questions: (1) the demonstration that low-copy GlyRs are present at inhibitory synapses in the hippocampus, (2) the sub-region specific expression and functional role of GlyRs in the ventral versus dorsal striatum.

The following review was provided later under the name “Reviewer #4”. To avoid confusion with the last reviewer from above we will refer to this review as R4-2.

> ***Reviewer #4-2 (Evidence, reproducibility and clarity):***
>
> *Summary:*
>
> *Provide a short summary of the findings and key conclusions (including methodology and model system(s) where appropriate).*
>
> *The authors investigate the presence of synaptic glycine receptors in the telencephalon, whose presence and function is poorly understood.*
>
> *Using a transgenically labeled glycine receptor beta subunit (Glrb-mEos4b) mouse model together with super-resolution microscopy (SLMM, dSTORM), they demonstrate the presence of a low but detectable amount of synaptically localized GLRB in the hippocampus. While they do not perform a functional analysis of these receptors, they do demonstrate that these subunits are integrated into the inhibitory postsynaptic density (iPSD) as labeled by the scaffold protein gephyrin. These findings demonstrate that a low level of synaptically localized glycerine receptor subunits exist in the hippocampal formation, although whether or not they have a functional relevance remains unknown.*
>
> *They then proceed to quantify synaptic glycine receptors in the striatum, demonstrating that the ventral striatum has a significantly higher amount of GLRB co-localized with gephyrin than the dorsal striatum or the hippocampus. They then recorded pharmacologically isolated glycinergic miniature inhibitory postsynaptic currents (mIPSCs) from striatal neurons. In line with their structural observations, these recordings confirmed the presence of synaptic glycinergic signaling in the ventral striatum, and an almost complete absence in the dorsal striatum. Together, these findings demonstrate that synaptic glycine receptors in the ventral striatum are present and functional, while an important contribution to dorsal striatal activity is less likely.*
>
> *Lastly, the authors use existing mRNA and protein datasets to show that the expression level of GLRA1 across the brain positively correlates with the presence of synaptic GLRB.*
>
> *The authors use lentiviral expression of mEos4b-tagged glycine receptor alpha1, alpha2, and beta subunits (GLRA1, GLRA1, GLRB) in cultured hippocampal neurons to investigate the ability of these subunits to cause the synaptic localization of glycine receptors. They suggest that the alpha1 subunit has a higher propensity to localize at the inhibitory postsynapse (labeled via gephyrin) than the alpha2 or beta subunits, and may therefore contribute to the distribution of functional synaptic glycine receptors across the brain.*
>
> *Major comments:*
>
> *- Are the key conclusions convincing?*
>
> *The authors are generally precise in the formulation of their conclusions.*
>
> *(1) They demonstrate a very low, but detectable, amount of a synaptically localized glycine receptor subunit in a transgenic (GlrB-mEos4b) mouse model. They demonstrate that the GLRB-mEos4b fusion protein is integrated into the iPSD as determined by*

> *gephyrin labelling. The authors do not perform functional tests of these receptors and do not state any such conclusions.*
>
> *(2) The authors show that GLRB-mEos4b is clearly detectable in the striatum and integrated into gephyrin clusters at a significantly higher rate in the ventral striatum compared to the dorsal striatum, which is in line with previous studies.*
>
> *(3) Adding to their quantification of GLRB-mEos4b in the striatum, the authors demonstrate the presence of glycinergic miniature IPSCs in the ventral striatum, and an almost complete absence of mIPSCs in the dorsal striatum. These currents support the observation that GLRB-mEos4b is more synaptically integrated in the ventral striatum compared to the dorsal striatum.*
>
> *(4) The authors show that lentiviral expression of GLRA1-mEos4b leads to a visually higher number of GLR clusters in cultured hippocampal neurons, and a co-localization of some clusters with gephyrin. The authors claim that this supports the idea that GLRA1 may be an important driver of synaptic glycine receptor localization. However, no quantification or statistical analysis of the number of puncta or their colocalization with gephyrin is provided for any of the expressed subunits. Such a claim should be supported by quantification and statistics*

A thorough analysis and quantification of the data in Fig.5 has been carried out as requested by all the other reviewers (e.g. R1, point 3). The new data and results have been described in the revised manuscript (pp. 9-10, 13-14).

> *- Should the authors qualify some of their claims as preliminary or speculative, or remove them altogether?*
>
> *One unaddressed caveat is the fact that a GLRB-mEos4b fusion protein may behave differently in terms of localization and synaptic integration than wild-type GLRB. While unlikely, it is possible that mEos4b interacts either with itself or synaptic proteins in a way that changes the fused GLRB subunit's localization. Such an effect would be unlikely to affect synaptic function in a measurable way, but might be detected at a structural level by highly sensitive methods such as SMLM and STORM in regions with very low molecule numbers (such as the hippocampus). Since reliable antibodies against GLRB in brain tissue sections are not available, this would be difficult to test. Considering that no functional measures of the hippocampal detections exist, we would suggest that this possible caveat be mentioned for this particular experiment.*

This question has also been raised before (R1, point 5). According to an earlier study the mEos4b-GlyRb knock-in does not cause any obvious phenotypes, with the possible exception of minor loss of glycine potency (Maynard et al. 2021 eLife). The fact that the synaptic levels in the spinal cord in heterozygous animals are precisely half of those of homozygous animals argues against differences in receptor expression, heteropentameric assembly, forward trafficking to the plasma membrane and integration into the synaptic membrane as confirmed using quantitative super-resolution CLEM (Maynard et al. 2021 eLife). Accordingly, we did not observe any behavioural deficits in these animals, making it a powerful experimental model. We have added this information in the revised manuscript (p. 4).

> *In addition, without any quantification or statistical analysis, the author's claims regarding the necessity of GLRA1 expression for the synaptic localization of glycine receptors in cultured hippocampal neurons should probably be described as preliminary (Fig. 5).*

As mentioned before, we have substantially revised this part (R1, point 3). The quantification and analysis in the new Fig. 5 support our earlier interpretation.

> *- Would additional experiments be essential to support the claims of the paper? Request additional experiments only where necessary for the paper as it is, and do not ask authors to open new lines of experimentation.*
>
> *The authors show that there is colocalization of gephyrin with the mEos4b-GlyRβ subunit using the Dual-colour SMLM. This is a powerful approach that allows for a claim to be made on the synaptic location of the glycine receptors. The images presented in Figure 1, together with the distance analysis in Figure 2, display the co-localization of the fluorophores. The co-localization images in all the selected regions, hippocampus and striatum, also show detections outside of the gephyrin clusters, which the authors refer to as extrasynaptic. These punctated small clusters seem to have the same size as the ones detected and assigned as part of the synapse. It would be informative if the authors analysed the distribution, density and size of these nonsynaptic clusters and presented the data in the manuscript and also compared it against the synaptic ones. Validating this extrasynaptic signal by staining for a dendritic marker, such as MAP-2 or maybe a somatic marker and assessing the co-localization with the non-synaptic clusters would also add even more credibility to them being extrasynaptic.*

The existence of extrasynaptic GlyRs is well attested in spinal cord neurons (e.g. Specht et al. 2013 Neuron; this study see Fig. S2). The fact that these appear as small clusters of detections in SMLM recordings results from the fact that a single fluorophore can be detected several times in consecutive image frames and because of blinking. Therefore, small clusters of detections likely represent single GlyRs (that can be counted), and not assemblies of several receptor complexes. Due to their diffusion in the neuronal membrane, they are seen as diffuse signals throughout the somatodendritic compartment in epifluorescence images (e.g. Fig. 5A). SMLM recordings of the same cells resolves this diffuse signal into discrete nanoclusters representing individual receptors (Fig. 5B). It is not clear what information co-localisation experiments with specific markers could provide, especially in hippocampal neurons, in which the copy numbers (and density) of GlyRs is next to zero.

> *In addition we would encourage the authors to quantify the clustering and co-localization of virally expressed GLRA1, GLRA2, and GLRB with gephyrin in order to support the associated claims (Fig. 5). Preferably, the density of GLR and gephyrin clusters (at least on the somatic surface, the proximal dendrites, or both) as well as their co-localization probability should be quantified if a causal claim about subunit-specific requirements for synaptic localization is to be made.*

Quantification of the data have been carried out (new Fig.5C,D). The results have been described before (R1, point 3) and support our earlier interpretation of the data (pp. 13-14).

> *Lastly, even though it may be outside of the scope of such a study analysing other parts of the hippocampal area could provide additional important information. If one looks at the Allen Institute's ISH of the beta subunit the strongest signal comes from the stratum oriens in the CA1 for example, suggesting that interneurons residing there would more likely have a higher expression of the glycine receptors. This could also be assessed by looking more carefully at the single cell transcriptomics, to see which cell types in the hippocampus show the highest mRNA levels. If the authors think that this is too much additional work, then perhaps a mention of this in the discussion would be good.*

We have added the requested information from the ISH database of the Allen Institute in the discussion as suggested by the reviewer (p. 12). However, in combination with the transcriptomic data (Fig. S1) our finding strongly suggest that the expression of synaptic GlyRs depends on the availability of alpha subunits rather than on the presence of the GlyRb transcript. This is obvious when one compares the mRNA levels in the hippocampus with those in the basal ganglia (striatum) and medulla. While the transcript concentrations of

GlyRb are elevated in all three regions and essentially the same, our data show that the GlyRb copy numbers at synapses differ over more than 2 orders of magnitude (Fig. 1B, Table 1).

> *- Are the suggested experiments realistic in terms of time and resources? It would help if you could add an estimated cost and time investment for substantial experiments.*
>
> *Since the labeling and some imaging has been performed already, the requested experiment would be a matter of deploying a method of quantification. In principle, it should not require any additional wet-lab experiments, although it may require additional imaging of existing samples.*
>
> *- Are the data and the methods presented in such a way that they can be reproduced?*
>
> *Yes, for the most part.*
>
> *- Are the experiments adequately replicated and statistical analysis adequate?*
>
> *Yes*
>
> *Minor comments:*
>
> *- Specific experimental issues that are easily addressable.*
>
> *N/A*
>
> *- Are prior studies referenced appropriately?*
>
> *Yes*
>
> *- Are the text and figures clear and accurate?*
>
> *Yes, although quantification in figure 5 is currently not present.*

A quantification has been added (see R1, point 3).

> *- Do you have suggestions that would help the authors improve the presentation of their data and conclusions?*
>
> *This paper presents a method that could be used to localize receptors and perhaps other proteins that are in low abundance or for which a detailed quantification is necessary. I would therefore suggest that Figure S4 is included into Figure 2 as the first panel, showcasing the demixing, followed by the results.*

We agree in principle with this suggestion. However, the revised Fig. S4 is more complex and we think that it would distract from the data shown in Fig. 2. Given that Fig. S4 is mostly methodological and not essential to understand the text, we have kept it in the supplement for the time being. We leave the final decision on this point to the editor.

> ***Reviewer #4-2 (Significance):***
>
> *[This review was supplied later]*
>
> *- Describe the nature and significance of the advance (e.g. conceptual, technical, clinical) for the field.*
>
> *Using a novel and high resolution method, the authors have provided strong evidence for the presence of glycine receptors in the murine hippocampus and in the dorsal striatum. The number of receptors calculated is small compared to the numbers found in the ventral striatum. This is the first study to quantify receptor numbers in these region. In addition it also lays a roadmap for future studies addressing similar questions.*

> *- Place the work in the context of the existing literature (provide references, where appropriate).*
>
> *This is done well by the authors in the curation of the literature. As stated above, the authors have filled a gap in the presence of glycine receptors in different brain regions, a subject of importance in understanding the role they play in brain activity and function.*
>
> *- State what audience might be interested in and influenced by the reported findings.*
>
> *Neuroscientists working at the synaptic level, on inhibitory neurotransmission and on fundamental mechanisms of expression of genes at low levels and their relationship to the presence of the protein would be interested. Furthermore, researchers in neuroscience and cell biology may benefit from and be inspired by the approach used in this manuscript, to potentially apply it to address their own aims.*

We thank the reviewer for the positive assessment of the technical and biological implications of our work, as well as the interest of our findings to a wide readership of neuroscientists and cell biologists.

> *- Define your field of expertise with a few keywords to help the authors contextualize your point of view. Indicate if there are any parts of the paper that you do not have sufficient expertise to evaluate.*
>
> *Synaptic transmission, inhibitory cells and GABAergic synapses functionally and structurally, cortex and cortical circuits. No strong expertise in super-resolution imaging methods.*

https://doi.org/10.7554/eLife.109447.1.sa0